AR92

ANNEX IV

GRANT NO. DE-FG22-89BC14444

DOE/BC/14444--14

DE93 012803

1990-1991 ANNUAL REPORT

RELATING TO FOSSIL ENERGY RESOURCE CHARACTERIZATION, RESEARCH, TECHNOLOGY DEVELOPMENT, AND TECHNOLOGY TRANSFER

between the

UNITED STATES DEPARTMENT OF ENERGY

and

THE STATE OF TEXAS

on

OIL RECOVERY ENHANCEMENT FROM FRACTURED, LOW PERMEABILITY RESERVOIRS

submitted by

TEXAS A&M UNIVERSITY

Principal Investigator

S. W. POSTON

DISCLAIMER

OIL RECOVERY ENHANCEMENT FROM FRACTURED, LOW PERMEABILITY RESERVOIRS

Contract No. DE-FG07-89BC14444

Texas A&M University
College Station, TX.

Contract Date: June 13, 1989
Anticipated Completion: Sept. 1, 1992
Government Award: $256,000
(Current Year)

Principal Investigator:
S. Poston

Project Manager
R. Lindsey
Bartlesville, Office

Reporting Period: 10/01/90 - 09/31/91

Table of Contents

1990 - 1991 Annual Report

A Study of Oil Recovery Enhancement from Fractured, Low Permeability Reservoirs
Specific Study Objective - The Austin Chalk Producing Trend

1.0 - Abstract

The results of the investigative efforts for this jointly funded DOE-State of Texas research project achieved during the 1990-1991 year may be summarized as follows:

Geological Characterization - Detailed maps of the development and hierarchical nature the fracture system exhibited by Austin Chalk outcrops were prepared. The results of these efforts were directly applied to the development of production decline type curves applicable to a dual-fracture-matrix flow system. Analysis of production records obtained from Austin Chalk operators illustrated the utility of these type curves to determine relative fracture/matrix contributions and extent.

Well-log response in Austin Chalk wells has been shown to be a reliable indicator of organic maturity.

Shear-wave splitting concepts were used to estimate fracture orientations from Vertical Seismic Profile, *VSP* data. Several programs were written to facilitate analysis of the data. The results of these efforts indicated fractures could be detected with *VSP* seismic methods.

Development of the EOR Imbibition Process - Laboratory displacement as well as Magnetic Resonance Imaging, *MRI* and Computed Tomography, *CT* imaging studies have shown the carbonated water-imbibition displacement process significantly accelerates and increases recovery from oil saturated, low permeability rocks.

The application of a cyclic carbonated water imbibition process, followed by reducing the pressure below the bubble point of the CO_2-water solution, indicated the possibility of alternate and new enhanced oil recovery method. The installation of an artificial solution gas drive significantly increased oil recovery.

The extent and arrangement of micro-fractures in Austin Chalk horizontal cores was mapped with *CT* scanning techniques. The degree of interconnection of the micro-fractures was easily visualized.

Both the semi-analytical and numerical models for studying the imbibition flooding method have been developed. Model testing is continuing.

Transfer of Technology - A number of presentations and publications were made at technical meetings and symposia. A transfer of technology conference concerning the results of our investigative efforts on the Austin Chalk was scheduled to be held on the Texas A&M University campus in early 1992.

Field Tests - Two operators amenable to conducting a carbonated water flood test on an Austin Chalk well have been identified. Feasibility studies are presently underway.

2.0 - Introduction

A multi-disciplinary investigation to develop innovative methods to characterize and to enhance oil recovery from dual porosity, fractured, low matrix permeability oil reservoirs has been conducted for the last two years. The Austin Chalk producing horizon trending through Texas was selected as the candidate for analysis.

Two major technological problems characteristic of the Austin Chalk as well as to other dual porosity reservoir types.

- *Reservoir Description* - Commercial oil production is dependent on the wellbore encountering a significant number of essentially vertical trending natural fractures. The prediction of the location and frequency of natural fractures at any particular region in the subsurface is generally problematical, unless extensive and detailed seismic data is available. Generally moderate to poor economic return on investment precludes acquisition of detailed seismic data for the average Austin Chalk operator.
- *Enhanced Oil Recovery* - A major portion of the oil remains in the low permeability matrix blocks after depletion. Primary production is derived mainly from the higher permeability fracture system. There are no economically realistic secondary or enhanced recovery methods currently available to mobilize a significant portion of this bypassed oil.

The following multi-faceted study was designed to develop new methods for reservoir description and enhancing recovery from the Austin Chalk producing trend. Tasks and respective investigators are listed in the following:

Reservoir Description

Task 1: Interpreting and Predicting Natural Fractures

Geological Studies - Dr. Friedman - Geology Department

Geophysical Studies - Dr. Gangi - Geophysical Department

Task 2: Relating Recovery to Well-log Signatures

Geological Studies - Dr. Berg - Geology Department

Petroleum Engineering Studies - Dr. Poston - Petroleum Engineering Department

Enhanced Oil Recovery

Task 3: Development of the EOR Imbibition Process

Laboratory Displacement Studies - Dr. Poston - Petroleum Engineering Department

Imaging Studies - Dr. Poston - Petroleum Engineering Department

Task 4 - Mathematical Modeling - Dr. Wu - Petroleum Engineering Department

Field Trials

Task 5 - Field Tests - Dr. Poston

Tasks 1 and 2 involve the development of better techniques for *Reservoir Description*, while Tasks 3 and 4 are concerned with the development of a new *Enhanced Oil Recovery* method. Task 5 is designed to apply these investigative efforts to the "real world" by finding operators to *Field Test* these new methods. The following discussion of the results of our investigations conducted during the 2nd year of the 3 year project is divided into these 3 major subjects of interest.

3.0 - Discussion of Research

3.1 - Reservoir Characterization

Characterization of Fractures in Outcrop - Dr. Friedman

The field phase of the characterization of fractures along the outcrop trend of the Austin Chalk has been completed. Fracture orientations and spacings particular to different deformational characteristics were mapped. Fig. 1 illustrates that fracturing in the Austin Chalk may be caused by the growth of anticlines, monoclinal flexures, normal or graben faults. The figure shows each structure produces essentially unique fracture patterns and distributions. Fracture distributions within differing geographical areas may differ by a considerable margin. Explorationists must be aware of the type of deformation prevalent in their area before predicting fracture distributions.

Detailed drawings at 1:12 to 1:48 scales were made of fracture traces on bedding planes mapped at Austin Chalk outcrops. An example of these efforts is shown in Fig. 2. Note the obvious hierarchical nature of the fracture arrangement. Major (macro) fractures are seen to trend in a roughly east-west manner, while subsidiary (2nd order) fractures intersect and connect the major fractures. Micro-fractures, subsidiary in size but genetically related to the 2nd order fractures are also present. The term "size" in this case infers fracture extent and width.

These fracture distribution data were studied to determine fracture length, orientation, and connectivity relationships. Fig. 3 is an example of some of these results. Note, the degree of regularity of these fracture relationships. The Austin Chalk fracture system appears to be well ordered and of a fractal geometry nature with a marginal degree of randomness.

Outcrop studies have shown the majority of the fractures terminate in zones where the clay/organic content of the chalk increases. Laboratory studies have shown Young's Modulus correlates strongly with rock strength, and rock strength correlates with fracture abundance when failure occurs in the brittle regime. Sonic and density logs might provide direct measures of rock strength in the brittle regime and hence of the fracturability of the rock if this fact is correct.

The key question in using data from outcrops to predict or model the potential of known naturally fractured reservoirs at depth deals with the degree to which outcrop data can be extrapolated to the subsurface. Plans have been made to study this critical problem with the aid of Schlumberger's Formation Microscanner data from the horizontal segments of wells drilled along the Austin Chalk trend.

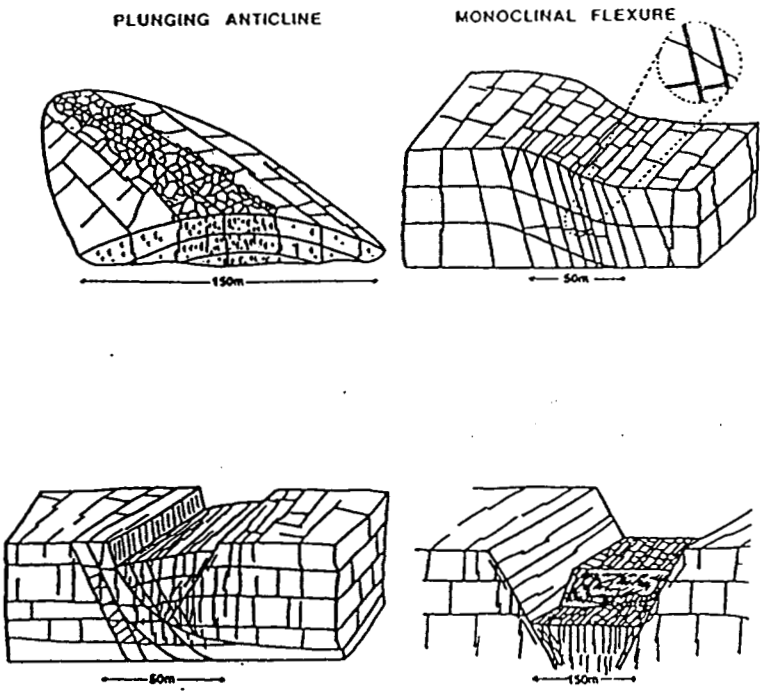

Fig. 1 - Schematic Illustration of the Four Structural Types and Their Associated Fractures

Scale: 1 in = 4 ft

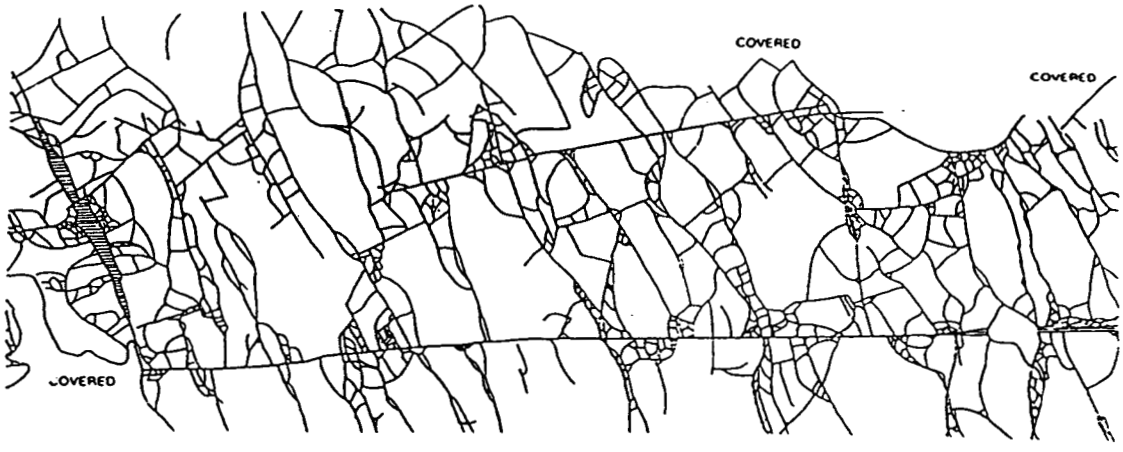

Fig. 2 - Example of Detailed Map of Fracture Traces

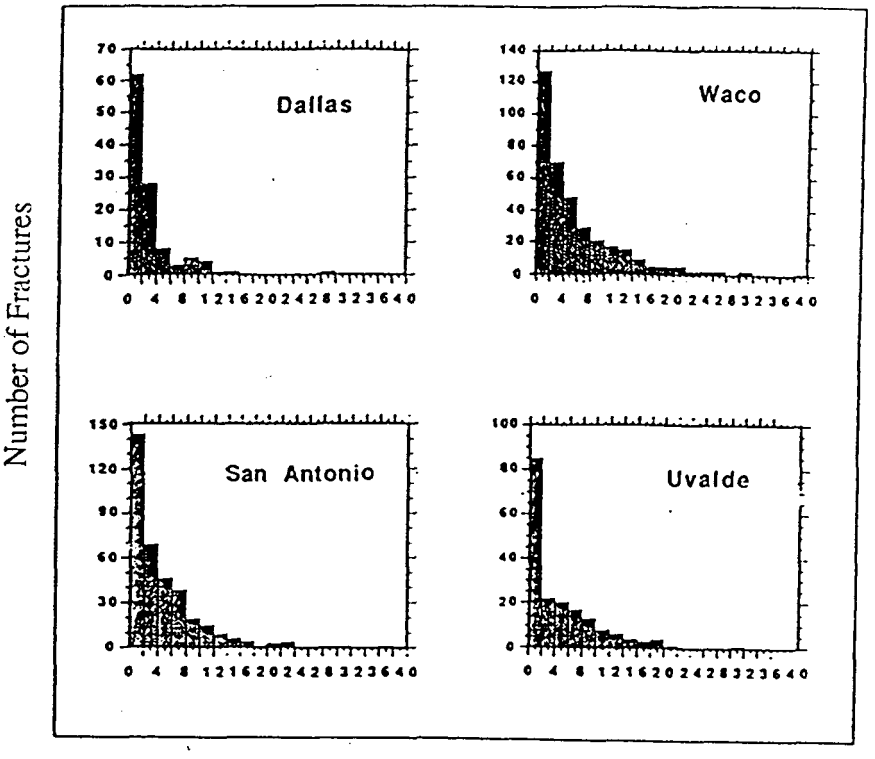

Fig. 3 - Plots Illustrating Fracture Spacing Data

Research by Hinds and Berg[1] conducted under the funding umbrella of Annex IV has shown it is possible use well log analysis to identify which intervals within a stratigraphic unit are most likely to be fractured. Research was conducted to determine if Young's Modulus correlates strongly with rock strength and to see if rock strength correlates with fracture abundance.

An earlier study[2] on the mechanical stratigraphy of the Austin chalk showed the upper (Big House Chalk) and lower (Atco Chalk) massive chalk members are the most fractured stratigraphic intervals observed at the outcrop. This point is in agreement with empirical evidence derived from analysis of drilling records. Moreover, it is known that rock fracturability in the brittle regime rock is largely a function of increasing strength which increases with decreasing porosity and decreasing clay (smectite) content. In fact, our

experimental deformation studies show that as little as 4% clay will decrease the rock sample strength from 30 to 42% when compared to specimens devoid of clay.

Data in the literature[3] indicate there is a strong correlation between Young's Modulus and compressive strength and tensile strength. Preliminary data of Austin Chalk rock samples obtained from the Pearsall Field, show a fair correlation between Young's Modulus and compressive strength and a reasonable correlation between normalized fracture length and distortional strain energy.

Transfer of Technology - The following is a listing of the presentations and publications pertaining to these subjects which were presented during the year.

1. Corbett, K.P., Friedman, M., Wiltschko, D.V., Hung, J., 1991a, Characteristics of natural fractures in the Austin chalk outcrop trend, p. 3 - 11 *in*, Stewart Chuber, Ed., *Proc. South Texas Geological Society Symposium on the Austin Chalk,* Feb. 25, 26, San Antonio, TX., 131 p.

2. Corbett, K.P., Friedman, M., Wiltschko, D. V.,and Hung, J.H., 1991b, Controls on fracture development, spacing, and geometry in the Austin Chalk formation, Central Texas: Considerations for Exploration and Production: *Dallas Geological Soc. Field Trip No. 4,* AAPG Ann. Conv., Dallas, Tx, April 1991, 49p.

3. Wiltschko, D. V., Corbett, K. P., Friedman, M., and Hung, J., in press, Predicting fracture connectivity and intensity within the Austin Chalk from outcrop fracture maps and scanline data, *Gulf Coast Association of Geol. Socs.*

Conclusions - The following conclusions may be derived from the studies conducted during the past year.

- Outcrop studies indicate there is an ordered and hierarchical nature to the Austin Chalk fracturing system observed in the outcrop.
- There is a definite correlation between rock brittleness and fracturability.

Future Efforts - Young's Modulus data obtained from sonic velocity measurements and strength data are to be added to the Austin Chalk data base. The ability to quantify the fracture surface area induced in experimentally deformed specimens as a measure of fracture abundance will be investigated. *CT* imaging is to be used in this regard. The *CT* data will be compared with the results obtained by optically measuring the fracture size. Stereological principles will be used to measure fracture surface area per unit volume.

Geophysical Studies - Dr. Gangi

Introduction - Shear waves (s-wave) may be split into components oriented in the 'fast' and 'slow' directions when propagating through an anisotropic medium. This splitting behavior is illustrated in Fig. 4. The horizontally polarized shear waves are seen to be travelling in the vertical direction in an elastic medium containing vertical fractures. The presence of the fractures will cause the shear waves whose motion is parallel to the faces of the fractures to possess a high speed. Shear waves whose motions are perpendicular to the fracture faces will have a lower speed. The fast and slow s-wave will be separated in time if the thickness of the fractured layer is sufficiently large.

Fig. 4 also shows that only the slow wave will be detected on a geophone oriented perpendicular to the fracture faces, or in the 'slow' direction. The fast waves may be detected by a geophone oriented parallel to the fracture faces, or in the 'fast' direction.

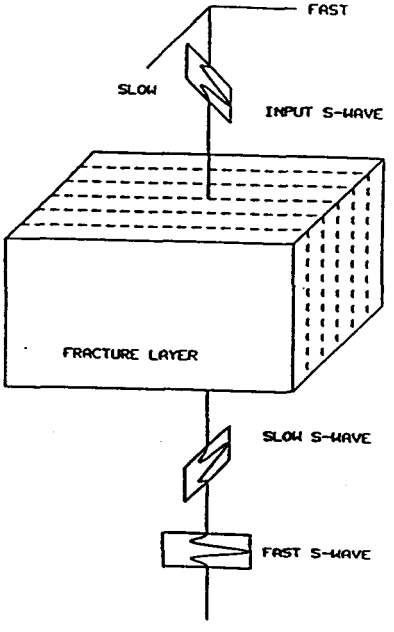

Fig. 4 - Shear-wave Splitting and Repolarization After Passing Through a Fractured Layer

The 'fast' and 'slow' orientations and the vertical direction constitute the principal axes. The orientation of the principal axes can be determined by finding the directions for the sources and geophones where there is no motion on the fast or slow geophone when the source is oriented in the slow or fast direction. The geophone and source pairs must be maintained perpendicular to each other and each geophone must be oriented parallel to one of the source directions.

There would be no motion on the geophone which is perpendicular to a horizontal source in an isotropic medium. The principal axes can have any orientation for an isotropic medium. An indication of an anisotropic medium is the detection of shear waves on geophones oriented perpendicular to the sources.

Preprocessing of Data - The data is usually read from the tapes and the traces are edited to eliminate bad traces. The data are then stacked and the signals for the horizontal, in-line or cross-line and vertical, downward sources are generated by subtracting and adding the traces.

An example of the results of performing these operations for the horizontal components is shown in Fig. 5. The data traces begin at 1600 ms where the direct s-waves begin. The p-waves occur at earlier times in the traces, but are not shown because only the s-waves are of interest when solving this particular problem. The s-wave wave forms are variable both in amplitude and time. These effects would be expected if the geophones are not oriented parallel and perpendicular to the source directions. The geophone can be oriented using the gyro data recorded for each geophone position.

The results obtained after 'gyro rotation' are shown in Fig. 6. Note the smooth variation of the first-arrival signals with depth. However, also note that the cross-diagonal components are not zero, as would be expected if the medium were isotropic. While some of the cross-diagonal signals may be caused by scattering from heterogeneities, the major part of these signals is derived by the anisotropy introduced by vertical fractures.

Hodograms were generated from these results. Fig. 7 is an example of some of the previously processed data. The hodograms are generated by the locus of the end of the vector obtained by the vector addition of the signals from the in-line and cross-line geophones. The hodograms would show rectilinear motion in the source direction only if the medium was isotropic. The motions for the cross-line source, in particular, are strongly non-rectilinear and neither hodogram is oriented in the direction of its source. This is a clear indication that anisotropy may exist.

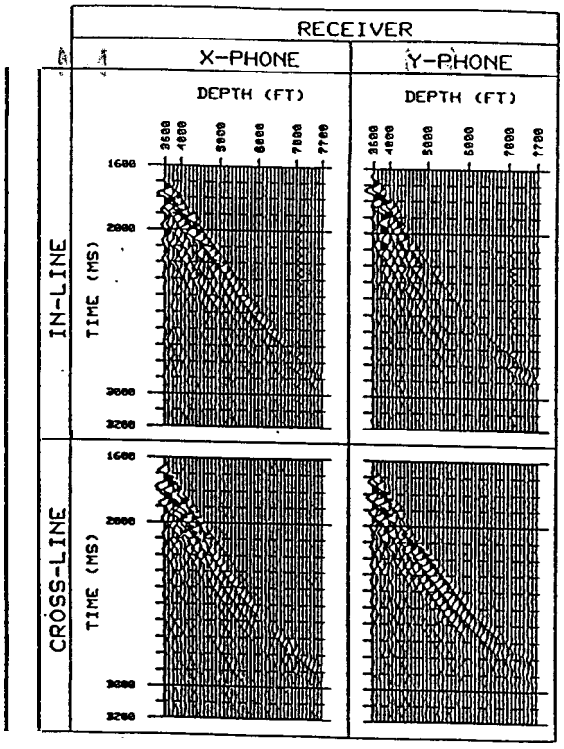

Fig. 5 - Edited and Stacked Traces Before Gyro Rotation

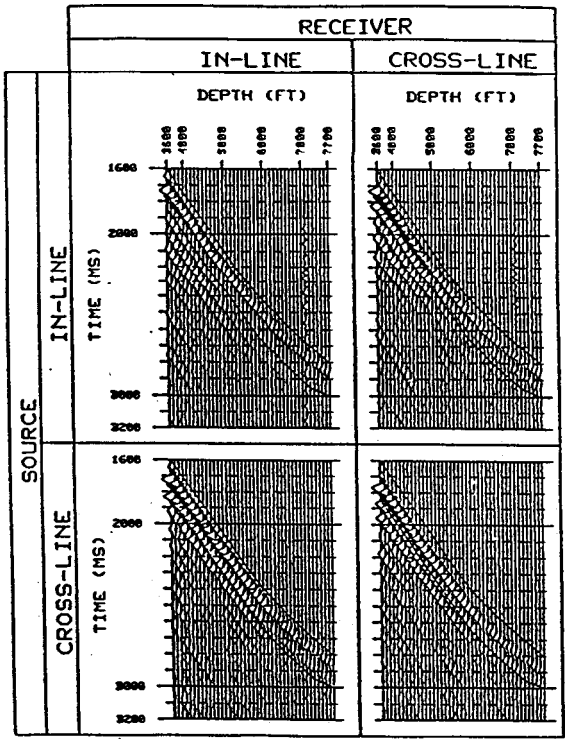

Fig. 6 - Edited and Stacked Traces After Gyro Rotation

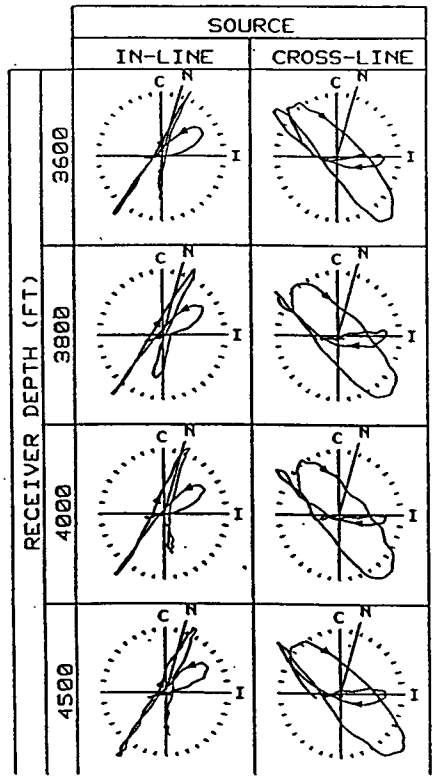

Fig. 7 - Hodograms Generated from Gyro Rotated Horizontal Components

Nine-component Vertical Seismic Profile, *VSP* data was processed during the past year. Programs were written to:

- Stack the VSP data, reorient the signals received from the down-hole geophones, and edit and filter the individual traces.
- Generate signals for in-line and cross-line sources.
- Rotate the source and geophone signals to the principal-axes orientations for the anisotropic, fractured medium. Use the orientations of the principal axes to determine the orientations of subsurface fractures.

The method used to determine the directions of the fractures (i.e., the principal axes for the anisotropy) is to rotate the four horizontal components of the signals to the principal directions. The cross-diagonal terms will be zero or, at least, minimized when the signals have been properly rotated.

The recorded displacement field is a function of, 1) the in-line geophone component for the in-line source, 2) the cross-line component for the in-line source, 3) the in-line

component for the cross-line source, and, 4) the cross-line component for the cross-line source. The (matrix) displacement field can be obtained after rotating both the sources and receivers.

Results of Analysis - The fracture orientations were determined by maximizing the ratio of the energy windows in the rotated, 'in-line, in-line' and 'in-line, cross-line' components. These orientations are shown as a solid line in Fig. 8. The angles obtained by maximizing the energy ratio are shown as the dashed line in Fig. 8. The asterisks on the depth axes indicate those depths for which the source location was changed. There is no strong correlation between the movement of the source truck and the variations in the determined fracture orientations. There are however, some small variations in the fracture orientation angle with depth. These effects will be discussed later. The measured fracture orientation is fairly constant with depth and is approximately N45°E. This is the inferred direction for the fracture planes.

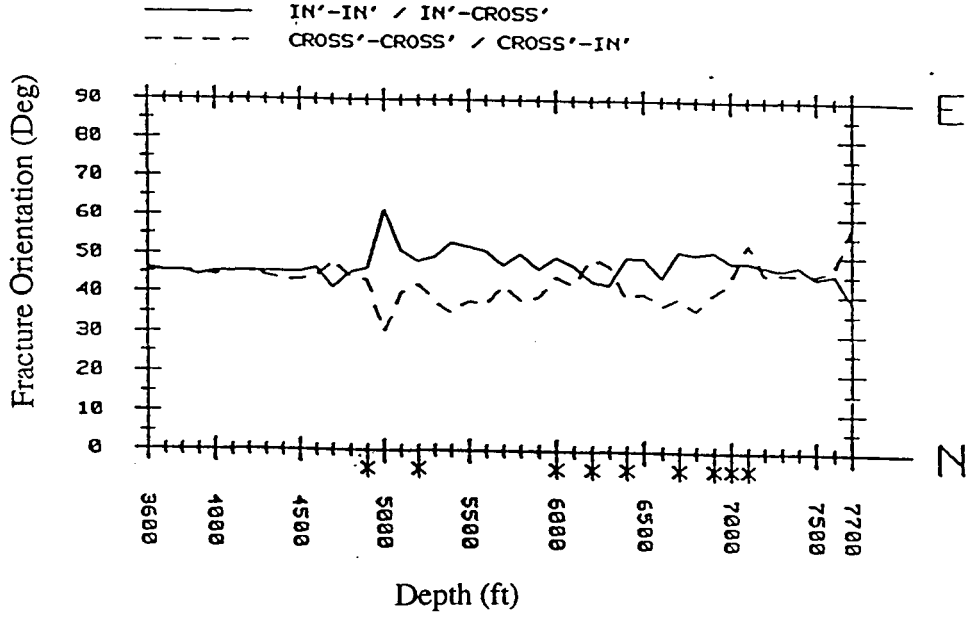

Fig. 8 - Fracture Orientations Determined by Maximizing the Diagonal Energies

Effects of Source Imbalance - The ratio of the energy values in the 200-msec window in the inferred fast direction to that in the inferred slow direction are illustrated in Fig. 9. The energy ratio varies in fairly constant terms for all depths except at 5,000 and 7,100 ft. where large deviations occur. These are also the depths for which there are large deviations

in the fracture orientations observed in Fig. 8. The amplitudes for the in-line source were found to be small for the 5,000 ft depth compared to the other depths, while the signals at 7,100 ft for the in-line source are nosier than seen in other traces. We concluded that the differences or imbalances in the in-line and cross-line sources for the 5,000 ft depth was the source of the large variability in the orientation at that depth.

The variation of the fracture orientation decreased substantially when the source strengths at 5,000 ft were equalized by increasing the signal level in both the in-line and cross-line components for the in-line source. Similar equalizations were performed for the traces corresponding to the other depths. The results for the fracture orientations after source balancing are shown in Fig. 10. Note, the variability in the fracture orientation is considerably decreased by this simple balancing procedure. The large variation persists for the 7,100-ft depth because of the the noise in the in-line-source traces. The resulting 'average' fracture orientation is about N45°E.

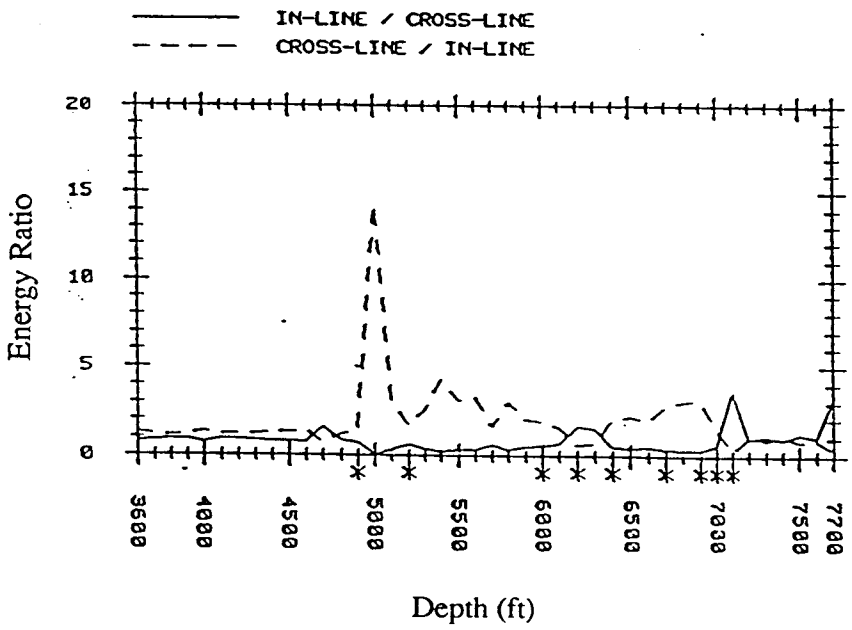

Fig. 9 - Ratio of Diagonal Energies As a Function of Depth

The time delay between the fast-fast component and the slow-slow component after source balancing for all depths is shown in Fig. 11. The average time delay is about 40 msec and remains relatively constant with depth. The time delay, is not unreasonable or unexpected since the sampling interval is 2 msec and that the frequency content in the signal peaks at about 10 Hz, with a variability of ± 4 msec in .

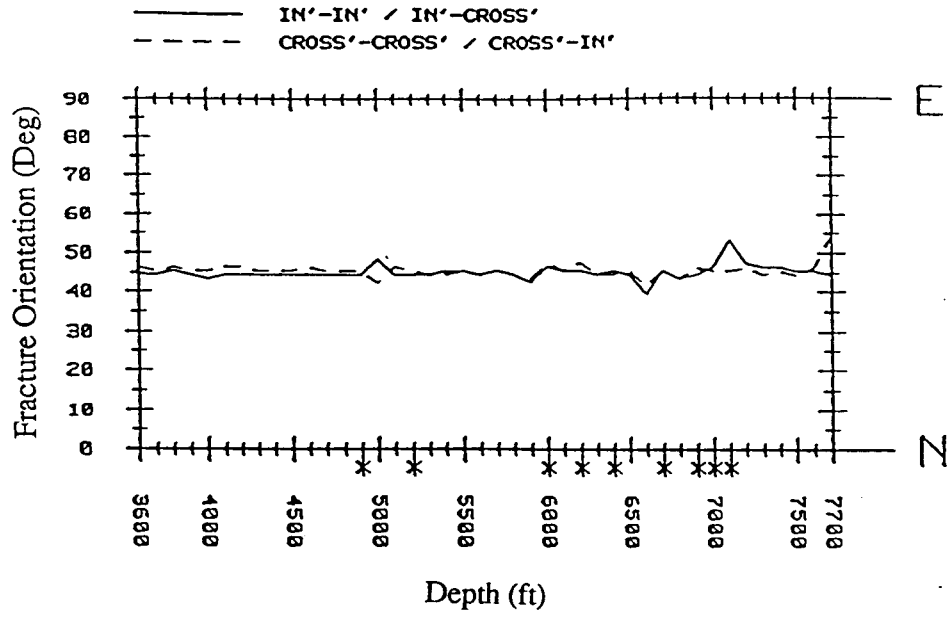

Fig. 10 - Fracture Orientations Obtained after Source Balancing

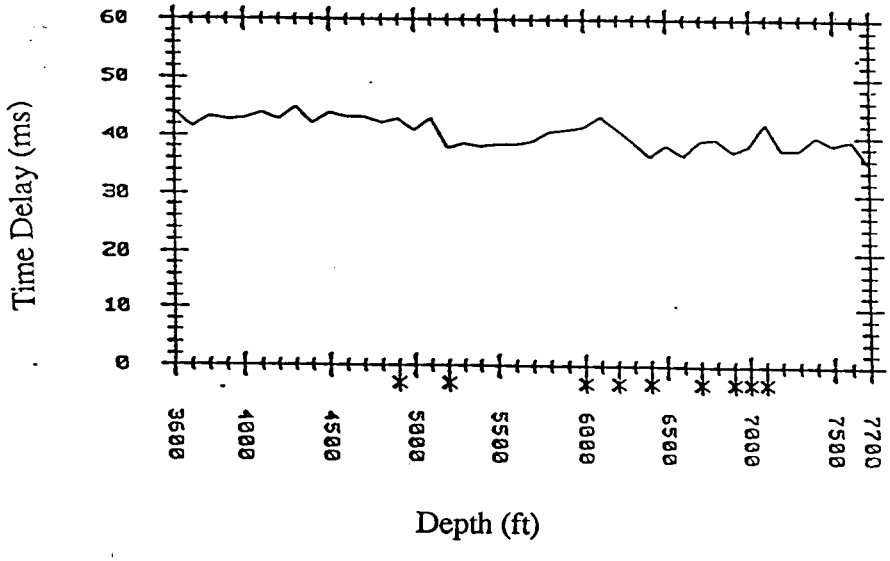

Fig. 11 - Time Delay Between the Fast and Slow Waves

The hodograms obtained for the rotated matrix of displacements at selected depths are shown in Fig. 12. The displacements are not only more rectilinear than those shown in Fig. 7, but they also are better aligned with the orientation of the sources. As in Fig. 7, the

hodograms are quite similar with depth. However, the motions for the 'fast' source are predominantly on the 'fast' geophone, while the motions for the 'slow' source are predominantly on the 'slow' geophone. There still are relatively large components in the cross directions. Again, we believe these 'large' cross components are due to source and geophone imbalances. We plan to try to eliminate them by compensating for/or equalizing these imbalances.

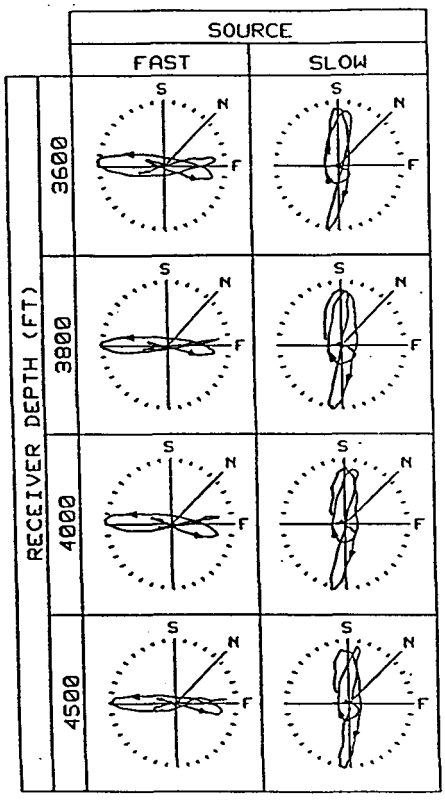

Fig. 12 - Hodograms of the Principle Components When the Sources are Rotated at the Principle Axis

Transfer of Technology - The following is a listing of the presentations and publications pertaining to these subjects which were presented during the year.

1. Choi, S., and, Gangi, A.F., (1991), "The Effect of Source Imbalances on the Determination of Fracture Orientation from VSP Data,". Presented at the 61st Annual Meeting of the Soc. Exploration Geophysists, held Nov 10-14, 1991 in Houston TX.

2. Hudgens, E., (1991), "Analysis of Vertical Resolution of Seismic Signals Associated with a Reservoir," M.S. Thesis, Dept. Geophysics, Texas A&M University, (Dec 1991).

Conclusions - The following conclusions may be derived from the studies conducted during the past year.

- The orientation of the fractures at the site location was found to be approximately N45°E.
- The bulk of the fractures at the site are located above 3,600 ft. There is no significant fracturing below this depth.
- The lack of perfectly rectilinear motion for the hodograms from sources oriented along the principal axes is due to imbalances in the source strengths and the geophone couplings. These imbalances lead to significant deviations in the determination of the fracture orientations. Methods for eliminating these imbalances are currently under investigation.

Future Efforts - Work is continuing on the VSP data set because studies conducted during the lst year of the project were not completed. These studies indicated errors in the fracture orientations were introduced because of imbalances in the sources.

Well Log - Productivity Relationships - Dr. Berg

The resistivity response to zones of organic maturity is a function of the value of the fluid saturations observed in the rock matrix. Oil generation in the Austin Chalk begins at 6,000 ft and 85°C according to geochemical studies.[4,5] Fig. 13 shows that the immature zone above 6,000 ft has essentially no oil saturation and about a 90% water saturation. The mature zone is divided into an upper storage zone and a lower migration zone. The storage zone from 6,000 to 7,000 ft contains greater than 60% oil saturation and 40% or less of water saturation. The migration zone below 7,000 ft contains 20% oil saturation and a 60% water saturation.

Bitumen is retained in the rock matrix of the storage zone because rock permeabilities are less than 0.01 md when oil generation begins. The matrix holds nearly all of the generated petroleum. The expansion of oil and gas induces microfactures to be

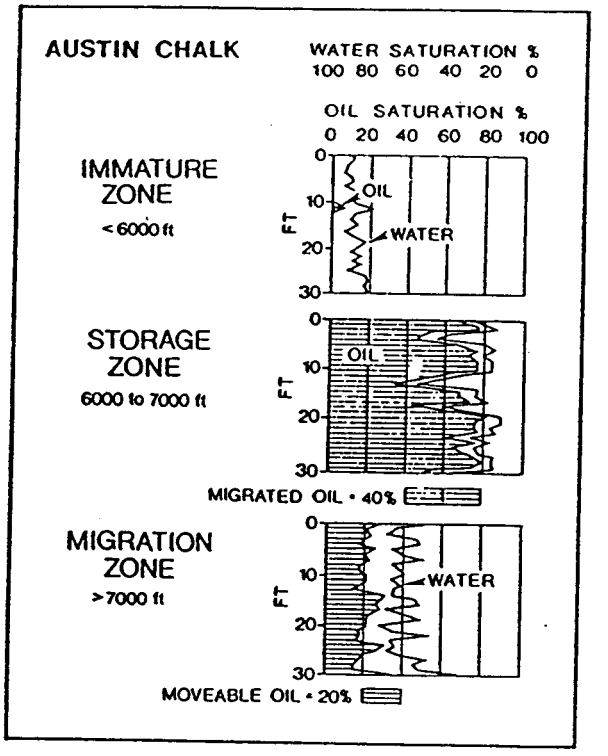

Fig. 13 - The Austin Chalk Oil Generation - Migration Model

formed. The formation of the micro-fractures allows the petroleum to escape from the matrix to nearby tectonic macro-fractures as well as allowing oil generation to continue. Consequently, the migration zone contains less oil and more water. The difference in water saturations between the storage and migration zones suggests that approximately 40% of the oil has migrated whereas about 20% remains in the matrix. The matrix oil appears to have been lost during core recovery and is interpreted to be moveable oil at subsurface conditions. Refer to Fig. 13. Thus, the migration zone contains about 40% of the generated oil in the tectonic fractures, while 20% remains trapped in the matrix.

Studies conducted under the umbrella of this research project have shown the average resistivity recorded in well logs directly reflects the water saturation[6]. The immature zone exhibits average resistivities of less than 10 ohm-m; the storage or accumulation zone exhibits resistivities greater than 40 ohm-m; and the migration zone exhibits resistivities in the intermediate range of 10 to 40 ohm-m. Consequently, it is possible to analysze resistivity logs to estimate the water saturation of a given interval and to predict whether the generated oil is largely retained in the matrix or has migrated to tectonic fractures.

The storage and migration zones are not controlled by depth alone, but depend on the quantity of petroleum which has been generated. Beds which contain a large amount of organic material generate larger amounts of petroleum at an early stage, and migration takes place near 7,000 ft. On the other had, beds which contain smaller amounts of organic material generate lesser amounts of petroleum. Migration takes place at somewhat greater depths. Therefore, the storage and migration of oil depends largely on organic richness.

The primary migration of oil from the low-permeability matrix to open tectonic fractures apprears to take place by means of micro-scale fractures formed during oil generation. The microfractures have been observed in cores of the Austin Chalk from the Pearsall field, Dimmitt County, South Texas. The lower part of the cored section shown in Fig. 14 is highly resistive and has an average oil saturation of about 60%. This section represents a storage zone of non-producible oil. No tectonic fractures were found in the core, and no production test was made of the section.

Microfractures were abundant at many levels in the core. The microfactures appear to be dissolution seams and are parallel to the bedding. Their widths are on the scale of micrometers. Truncated fossil fragments at the margins are primary evidence for dissolution. Thin section analysis indicates the microfactures are filled with a matrix of organic material, clay, pyrite, and other insolubles. Oil is present in discontinuous laminae within the matrix and suggests that the dissolution seams could provide the paths for primary migration of oil. A geochemical analysis will be made of selected samples in the storage interval to determine the maturity of organic matter and its relation to oil generation, saturation, and well-log response.

Field Applications of Study - The correlation of resistivity and fluid saturation suggests that resistivity also may be related to productivity. For example, true resistivity may reflect the relative amount of oil that has migrated from the rock matrix to tectonic fractures. High resistivity would indicate that oil is retained in the matrix whereas lower resistivity would suggest that most of the oil has migrated and now resides in nearby fractures where it is readily producible.

In order to test this hypothesis, a producing area in Pearsall field was selected for an initial study. Fig. 15 show the lease contains 6 producing wells and 1 dry hole. Wells 7, 8, 10, and 11 were vertical holes drilled and completed at an earlier date.

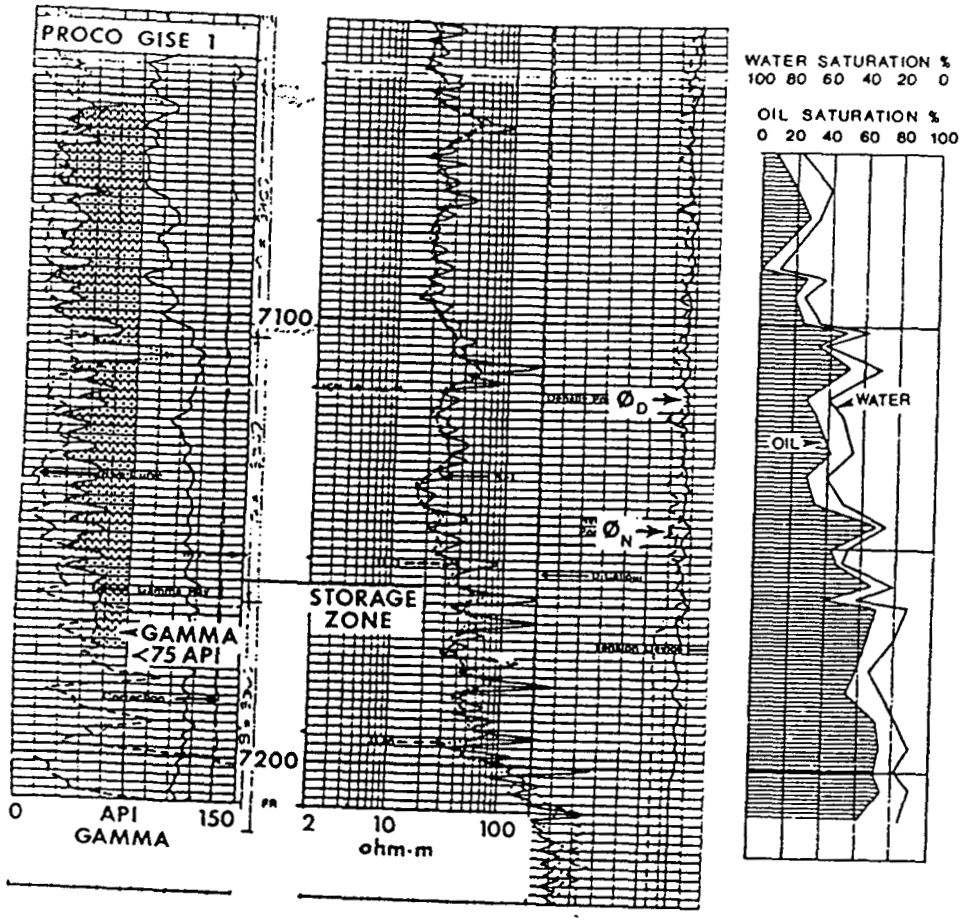

Fig. 14 - Log Section - PROCO Well

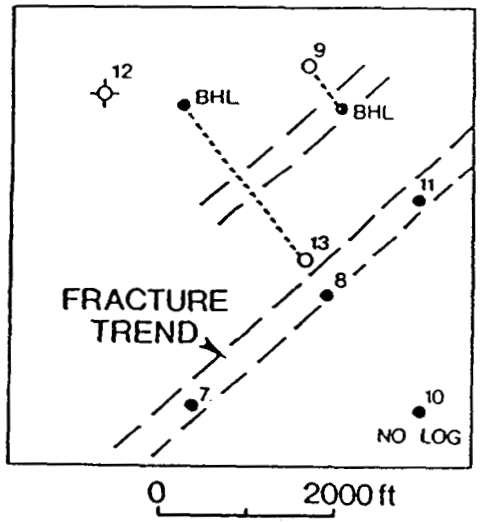

Fig. 15 - Location Map of the Pearsall Study Area

Well 9 is a short-radius horizontal well, and well 13 is a long-reach horizontal well. Well 12 is a vertical hole that was plugged and abandoned after producing less than 1,000 bbl of oil. Significant recoveries were reported for all of the other oil wells.

Fig. 16 shows that there is an inverse relationship of the initial potentials with the average resistivities measured across the perforated intervals. The resistivities are expressed as the product of average resistivity (R_t) times the height of the perforated section (h). The productive sections are in the lower part of the Austin and have nearly the same thickness of from 80 to 90 ft in each well.

Well 7 had the highest initial potential of 402 bbl/day and the lowest R_th value of 2,900 ohm-m-ft. Wells 11, 8, and 9 have successively lower potentials with increasing values of R_th. Well 12 had the lowest potential of 18 bbl/day and the highest R_th of 6000 ohm-m-ft. The interpretation of this relationship is that the section in well 12 retains a high saturation of matrix oil whereas in the other wells, larger and variable amounts of oil have been expelled to tectonic fractures.

There appears to be no correlation between cumulative production and resistivity for this geographical location in the Austin Chalk. The reason for this may be that the transmissibility of fractures encountered at the several locations are greatly different, and oil produced over a long time period reflects the characteristics of the fractures rather than the amount of oil expelled from the matrix. The results of the initial production study strongly suggests that well-log response can be related to productivity.

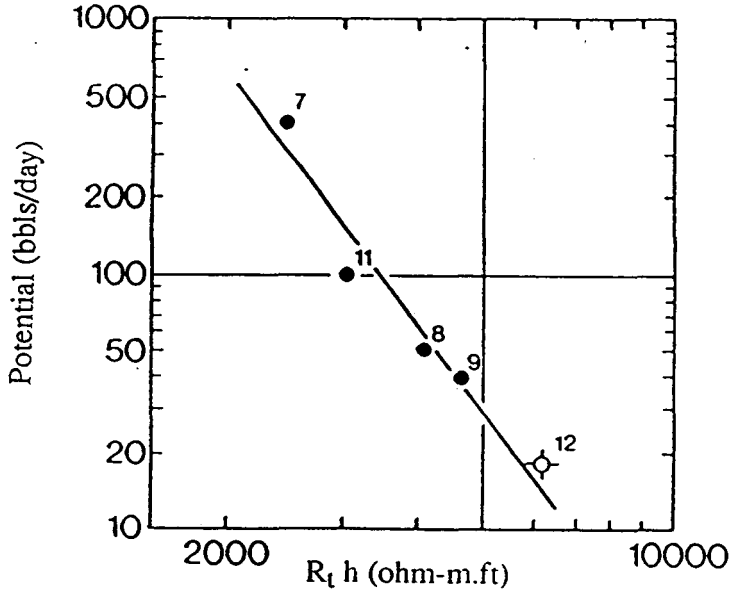

Fig. 16 - The Well Potential - Resistivity Plot

Transfer of Technology - The following is a listing of the presentations and publications pertaining to these subjects which were presented during the year.

1. Hinds, G.S., and R.R. Berg, (1990), "Estimating Organic Maturity from Well Logs, Upper Cretaceous Austin Chalk, Texas Gulf Coast": *Gulf Coast Association of Geological Societies Transactions*, v. 40, p. 295-300.

2. Sanford, J.R., (1990), "Well Productivity in the Austin Chalk": Master of Engineering Report, (May 1990) Texas A&M University.

Conclusions - Resistivity log response appears to be a reliable indicator of organic maturity in the Austin Chalk, and the resistivity response is largely dependent on the oil saturation in the matrix. Therefore, the productivity of wells also may be reflected in log response which in turn may be used as an aid in the prediction of well performance. Furthermore, the interpretation of microscale dissolution features in cores may shed light on the important problem of primary migration from source rock to reservoir.

Future Efforts - Well logs, completion histories, and oil production records have been gathered on more than 50 wells in the Giddings field, Burleson County, Texas. The well logs have been digitized, and average values of resistivity have been calculated through the producing intervals. Production decline curves will be interpreted to allocate production to fractures and matrix, and productivity of wells will be related to log response.

Decline Curve Studies - Dr. Chen

A naturally fractured reservoir is composed of a medium comprised of fracture and matrix blocks. The properties associated with each sub-medium are quite different. The fracture-matrix geometry and extent and connectivity of the system is quite complex and in most cases is definitely non-homogeneous. These features impose great difficulties in the modeling of a naturally fractured reservoir.

The first model describing fluid flow in naturally fractured reservoirs was presented by Barenblatt.[7,8] The fracture and matrix sub-media were treated as continua. Space and time fluid pressures corresponding to the fluid in the fracture and that in the matrix blocks was proposed. The fracture and matrix pressure fields are then superimposed and are coupled by using a fluid interchange term. No specific fracture-matrix geometries are assumed since the model scale is relatively large. A large scale causes the fracture-matrix geometries to lose their identities after the overlapping-continuum assumption is imposed.

Two major difficulties arise when the Barenblatt overlapping-continuum concept is applied to real cases:

- It is difficult to visualize two pressures at each point.
- The permeability required to calculate the flow rate is difficult to define since the two pressure fields are overlapped and may or may not be operating independently or co-dependently.

Barenblatt simplified his dual-continuum theory by neglecting the storage capability of the fractures and the macroscopic permeability of the matrix blocks. Refs. 9 and 10, attempted to refine Barenblatt's dual-porosity theory by applying a fluid interchange term. Wijesinghe and Culham[10] derived a generalized theory to relax the steady-type interporosity flow assumed by Barenblatt. Chen *et al.*[11] further simplified the theory and proposed an analytical, transient interporosity model. However, the inherent difficulties still remain since the main framework is based on Barenblatt's overlapping-continuum concept.

Another type of dual-porosity model requires an exact specification of fracture-matrix geometry.[13,14]. The problem essentially becomes not only tractable but also, in most cases, solvable when the exact inner structure of a fractured medium is specified. This is especially true for the modeling of the fluid interchange term. The inner structure is assumed to be homogeneous. A fractured medium is represented by certain simple repetitive patterns such as layered, cubic or spherical matrix blocks isolated by the fractures. The major difficulty of such exact geometry models is that the assumed fracture-matrix geometry may not be consistent with field observations.

Both overlapping-continuum and exact fracture-matrix geometry models involve a fracture-matrix fluid interchange term. A common and logical issue is how to "correctly" describe this term. Theoretically, the term is derived from a detailed reservoir description. In practice, however, the modeling of fluid interchange term *is the problem.*

Most research efforts concerning the modeling of naturally fractured reservoirs have more or less followed along these previously discussed lines. A completely different concept is explored in this study. The proposed concept has the following features:

- A single pressure field for each phase is assumed at each point
- No explicit fracture-matrix geometry is assumed.
- A fluid interchange term is not required.

Model Fundamentals - Darcy's Law is always associated with a porous volume in a macroscopically and statistically correct nature. The Darcy velocity term actually is a fictitious velocity averaged over the cross sectional area of the porous medium. It is not a true velocity within the pore. This statement implies that the nature of the permeability associated with the Darcy's Law and the validity of Darcy's Law depends on the defined pore volume.

Our approach is to use a modified form of Darcy's Law which takes into account the coexistence of fracture and matrix media with highly contrasting properties. As in the Barenblatt dual-continuum theory, the scale of the equation is sufficiently large to encompass two distinct types of media. Darcy's Law would still be valid if only one type of porous medium is considered. Therefore, we may say that this modified form of Darcy's Law is derived from the Darcy's Law.

The approach is different from that used by Barenblatt. However, a casual examination of the solutions presented by Barenblatt and that of the telegraph or wave type equations reveal certain similarities. This is probably due to the fact that a steady-type equation is used in developing our new modified Darcy's Law and in Barenblatt's fluid interchange term. We also note that by neglecting the terms with order greater than two in any dual-continuum PDE results in a form similar to our outcome. The exact relationship, however, is not immediately clear and is not identified at the present time.

Transfer of Technology - The following is a listing of the presentations and publications pertaining to this subject which was presented during the year.

1. Chen, H.Y., Poston, S.W. and Raghavan, R.: "The Well Response in a Naturally Fractured Reservoir: Arbitrary Fracture Connectivity and Unsteady Fluid Transfer," paper SPE 20566 presented at the 1990 Annual Technical Conference and Exhibition, New Orleans, LA, Sept. 23-26.

Conclusions - An approach using a modified Darcy's Law to model the naturally fractured reservoirs is proposed. The resulting governing partial differential equation using a modified form of Darcy's Law is a hyperbolic type equation. The development is highly heuristic. Justification from sound fundamental theory is still required. Also, the relationship between the proposed model and Barenblatt's must be identified.

Future Efforts - The proposed model does not consider explicit wellbore conditions such as wellbore storage, skin, and the effect of hydraulic fractures. The wellbore effects are

common in practice and affect the pressure and rate measurements at the wellbore, Future work should include including these effects in the model.

Field Case History Studies - Dr. Poston and Dr. Chen

Prediction of future production from a typical Austin Chalk well presents a particular problem because of the extreme heterogeneity of the producing system. The permeability of the matrix rock is on the order of 0.01 to 0.0001 md, while the fracture permeabilities usually range from 10 to 100 times greater. The productivity of an individual Austin Chalk well depends to a very great extent on the intensity of encountered fracture system, the extent of the natural fractures, and the permeability of matrix material. Estimation of remaining reserves and other reservoir characteristics is particularly difficult because of our inability to quantify the drainage character of the individual well. Additionally, most Austin Chalk wells are hydraulically fractured.

Well test and production records are usually the only information available for analyses. Therefore, decline curve analysis would be an obvious choice for predicting future production characteristics. The following section discusses the results of using type curves expressing dual fracture-matrix permeability flow to describe the drainage characteristics of Austin Chalk wells.

Fluid flow within this type of reservoir would be expected to be predominantly linear, not radial, since the major flow channels are fractures. Chen,[14] as a portion of the Annex IV research program developed production decline - type curves representing the expected flow characteristics from a dual fracture-matrix flow system. These type curves represent the expected producing characteristics for a reservoir possessing at least two different permeability fracture systems and a matrix block system are presented. A combination of flow through a major fracture system with infinite conductivity, linear flow through a set of lesser, subsidiary micro-fractures, and flow from the matrix block system into the micro-fracture system are represented by these curves.

The Geological Model - The work conducted by Dr. Friedman in the Outcrop - Subsurface portion of the Annex IV study showed the regularity of the patterns and fracturing system in a typical Austin Chalk section. Micro-fractures connect the major (macro)-fractures. There is a pronounced lessening of the fracture intensity away from the center of the flexure. The geological model explains why horizontal drilling has been such a success in the Austin Chalk.

Concepts derived from the geological study may be summarized as follows:

- Master(macro-) fractures have a periodic spacing with a common orientation and have a permeability significantly greater than that of the "minor" fractures.
- There is a set of "minor" fractures roughly aligned normal to the "master" fractures which connect the "master" fractures to each other.
- There is at least one other set of more subsidiary fractures which are more or less random in nature.

Figs. 17 and 18 are idealized representations of a typical Austin Chalk fracture system.

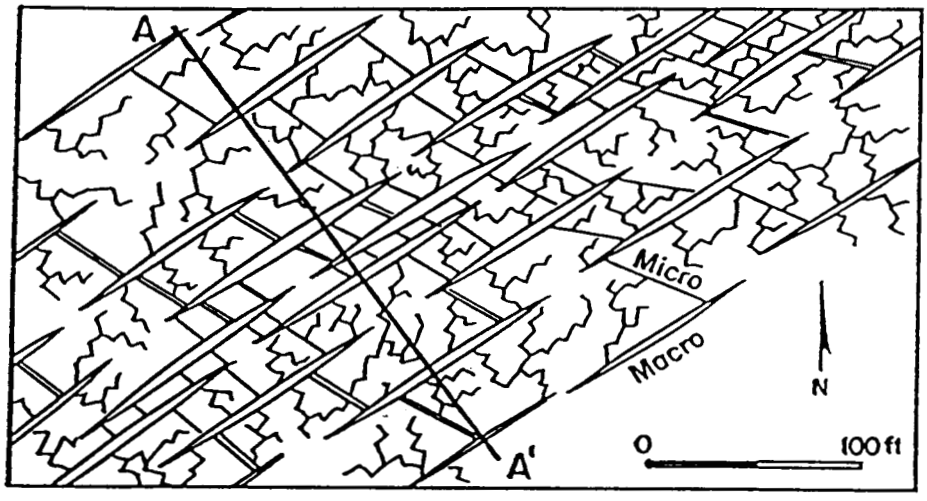

Fig. 17 - Idealized Macro- , Micro-Fracture and Matrix System - Plan View

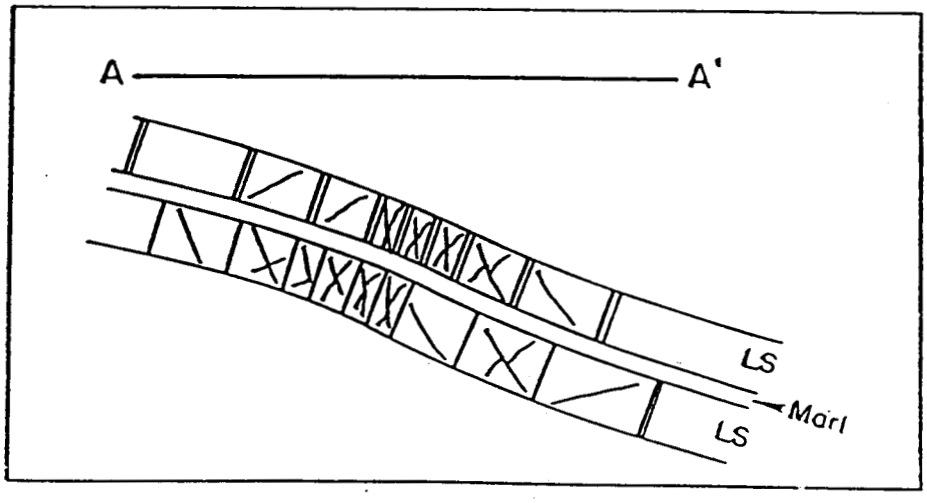

Fig. 18 - Idealized Macro and Micro-Fracture and Matrix System - Cross Section

Mathematical Model Considerations - The geological discussion indicates the fracture network is comprised of a dominant array of near-vertical macro-fractures. The micro-fractures supply varying degrees of interconnection between the macro-fractures.

A realistic mathematical model of the Austin Chalk must consider the spatially dependent fracture orientation, connectivity, distribution and intensity. Specifically, there is a necessity to distinguish macro- from micro-fractures when describing the producing characteristics of an Austin Chalk well.

A single-fracture type model is coupled to a dual-porosity type model. The following assumptions concerning the expected fracture characteristics and producing mechanisms are used to simplify the mathematical treatment.

- The macro-fractures deplete under essentially steady state conditions and are connected to the micro-fractures.
- The micro-fractures are more or less connected and are considered as a continuous network. Flow from the micro-fractures may be at transient or pseudosteady state conditions which subsequently feeds into the macro-fracture system. The matrix blocks are enclosed by the continuous fractures.
- Transient or pseudosteady state production from the matrix is fed into the micro-fractures. The matrix blocks act as supporting sources to feed the fractures with fluid.

The natural fracture network and matrix blocks are conceptualized as distinct, yet overlapping continua. The macroscopic flow pattern in the reservoir is represented by the flow in the natural fracture network superimposed by the flow system within the matrix blocks. Flow is from the fractured reservoir, into the wellbore intercepted fracture and then into the well.

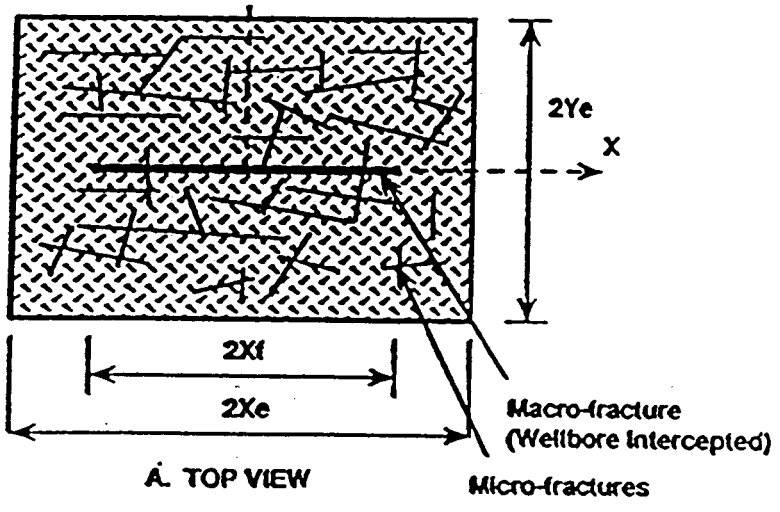

Fig. 19 - Model Elements

Fig. 19 is an idealized comparison of the macro- and micro-fractures and the flow supporting matrix. The initial decline is controlled by flow from the macro-fracture system, while late time flow is principally a function of the matrix properties. Early time macro-fracture flow would be expected to be essentially level since since the model defines this flow regime to be essentially steady state.

Type Curves - Dr. Chen

The type curves shown in Fig. 20 were constructed in a manner similar to the Fetkovich decline-type curves. A more extended discussion of the formulation of the type curves may be found in Ref. 14-17. The dimensionless parameters characterizing the dual fracture-matrix flow system are a storage-compressibility term, ω and a fracture extent term, γ.

The storage-compressibility term is defined as:

$$\omega = \frac{(\phi c_t)_f}{(\phi c_t)_f + (\phi c_t)_m} = \frac{(\phi c_t)_f}{(\phi c_t)_t}$$

The equation indicates ω is defined as the ratio of the storage-expansion values for the fracture system compared to that of the total system.

A high value of ω and homogeneous-reservoir-like production behavior would be an indication of poor fracture connectivity with relatively large matrix block sizes.

The fracture intensity term is defined as:

$$\gamma = (FI)^2 x_f^2 \frac{k_m}{k_f} \frac{(\phi c_t)_m}{(\phi c_t)_f} \beta_1 \beta_2 = \left(\frac{6}{\pi} \frac{y_e}{l_c}\right)^2 \frac{k_m}{k_f} \frac{(\phi c_t)_m}{(\phi c_t)_f}$$

where FI denotes the "Fracture Intensity" in terms of "number of fractures per foot" and l_c is the characteristic length of the matrix block. B_1 and B_2 are normalizing factors and are defined in Ref. 16.

The unique feature for the dual fracture-matrix type curve shown in Fig. 20 is the extended production tail. This production extension is a direct consequence of the matrix contribution in the dual-porosity formulation. Naturally fractured reservoirs with the permeability of the matrix block being to small to permit significant fluid migration to the micro-fractures should display a pronounced "fall off" late in the life of the well.

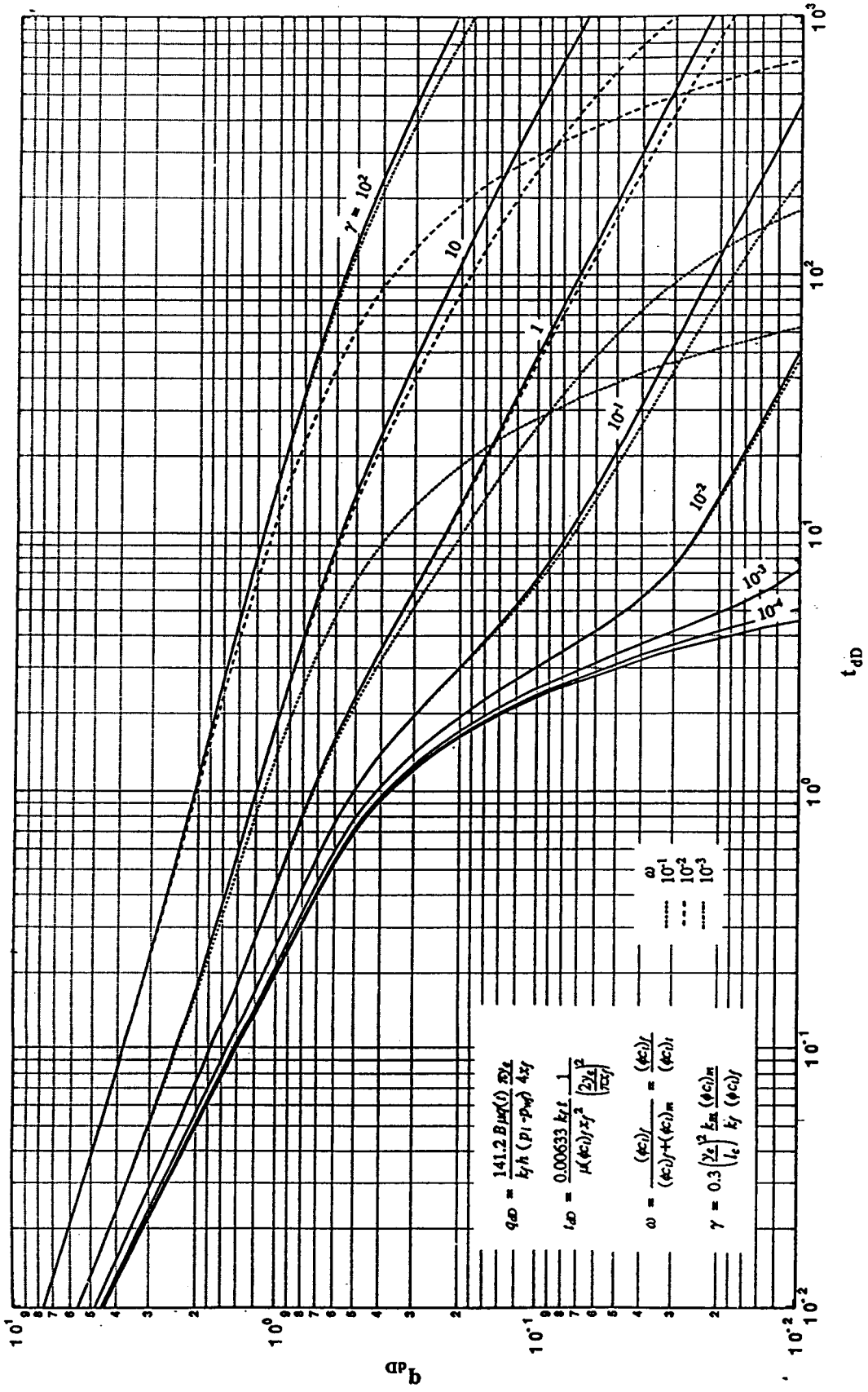

Fig. 20 - Chen Type Curves

In conclusion and for a *given* production rate:

• A large value of γ tends to be associated with small values of ω because fluid flow to the well is being maintained by the extended fracture system, not by maintenance of reservoir pressure due to a high storage value. Conversely,

• A small value of γ would have to be associated with large values of ω because the gas compressibility effect would have to be significant to maintain a comparable production rate. The implication of the foregoing analysis is that qualitative interpretation of more than one phase producing situations is realistic with these type curves even though the type-curves were generated with a single liquid solution. ω is generally low or liquid like (10^{-2} ~ 10^{-3}) range at initial conditions, .

Field Case Histories - Field case studies of production records from Austin Chalk, vertical and horizontal wells located in both the Pearsall and Giddings Fields illustrate the utility of the new, dual fracture-matrix concept to determine the variation of reservoir character, the degree of connectivity of offsetting wells as well as the ability to generate area wide "field" type curves.

The Bagget #8 Vertical Well - IP 67 BOPD on 01/79. Match characteristics - $\omega = <0.01$, $\gamma = 0.05$. The ω term was the same as for two adjacent wells, 7 and 9. Well 7 had been completed one year previous to the #8 well while the #8 well had been completed at approximately the same time as the #9 well. Oil production from the matrix is calculated to be 3,200 stb oil. Note, the significant difference in the levels between micro-fracture flow and matrix flow. All of the wells evaluated in this area showed this large difference in the two levels. There appears to be a significant difference between the micro-fracture and the matrix permeabilities. Fig. 21 presents the production curve match for the Bagget #8 well.

The Knesek A-1 Vertical Well - The well was drilled in late 1981. IP on 01/81 was 67 BOPD Match characteristics - $\omega = <0.01$, $\gamma = 0.05$. Note, the decline from micro-fracture flow to the matrix system appears to be essentially linear. This type of decline indicates the permeability of the micro-fracture and the matrix system are reasonably close to each other. Fig. 22 presents the production curve match.

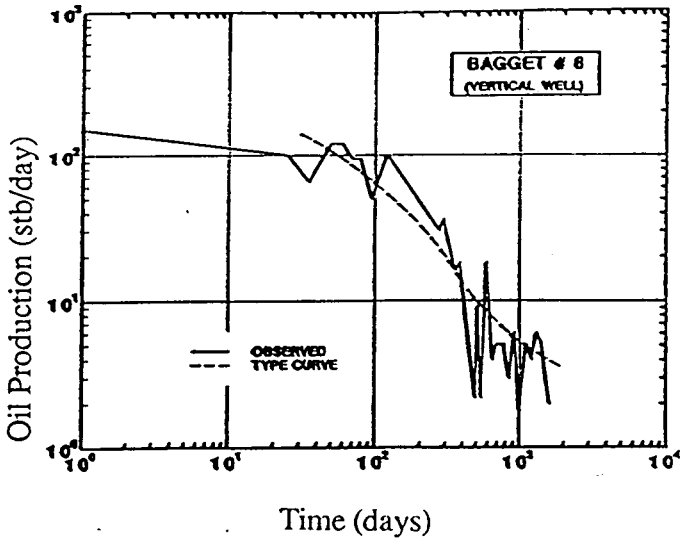

Fig. 21 - Initialized Decline Curve - Bagget No. 8 Well

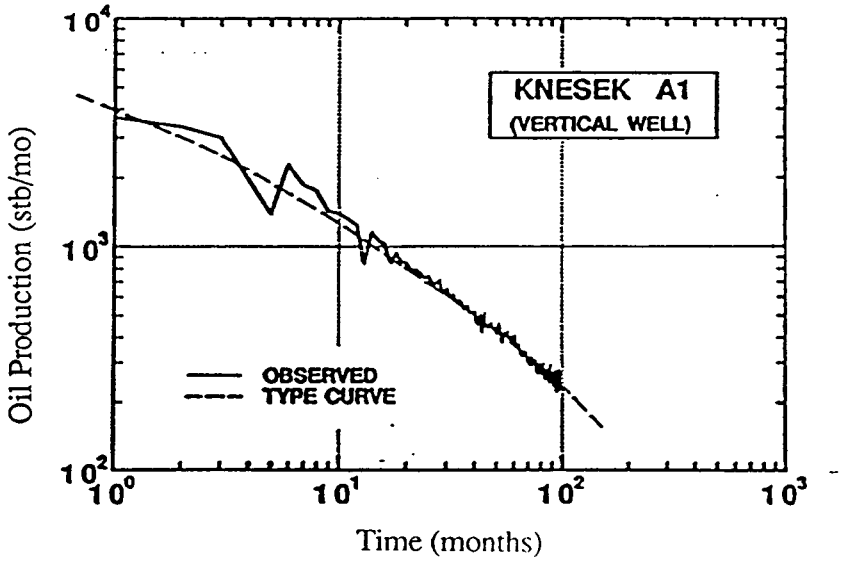

Fig. 22 - Initialized Decline Curve - Knesek A-1 Well

Family of Curves - Three Horizontal Wells - The A, B, and C wells were drilled and completed in 1990 and are adjacent to each other. The ω term was the same for the three wells, which indicates they are more than likely producing from the same drainage system. Well "A" appears to be producing from a lesser fracture system than is observed by the

other two wells even though its cumulative production is greater. Match points derived from Fig. 23 are listed in the following table.

Well	ω	γ	N_p
A	0.1	1	112,000
B	0.1	10	79,000
C	0.1	10	96,000

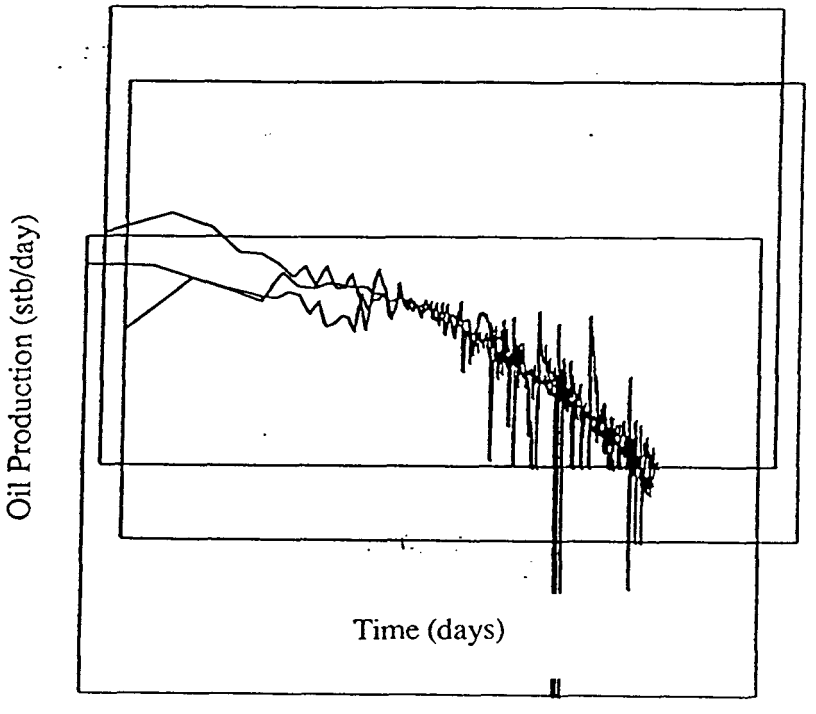

Fig. 23 - Family of Curves - Horizontal Wells

Transfer of Technology -The following is a listing of the presentation and publications pertaining to these subjects which were presented during the year.

1. Chen, H.Y., Raghavan, R., and Poston, S.W.,"An Application of the Product Solution Principal for Instantaneous Source and Green's Function in the Laplace Domain," *SPE Formation Evaluation.*(June 1991)

2. Poston, S.W., Chen, H.Y., and Sandford, J.R.,"Fitting Type Curves to Austin Chalk Wells," SPE 21653. Presented at the 1991 Production Operations Symposium, Oklahoma City, OK.

3. Chen, H.Y., Poston, S.W., and Raghavan, R.,"Mathematical Development of Austin Chalk Type Curves," paper SPE 23527 submitted for publication, Dec. 1991; accepted for publication.

4. Poston, S.W., Chen, H.Y., and Aly, A.,"Applying a Geological Model to the Formulation of Production Decline Type Curves in the Austin Chalk," Paper 3RC-74. Presented at the Third International Reservoir Characterization Technical Conference, November 3-5, 1991, Tulsa, OK.

Conclusions - Type curves representing flow equations describing a generalized geological model approximating the expected fracture network system within the Austin Chalk were formulated. The utility of the new method to differentiate between individual well producing characteristics has been illustrated by comparing decline curves from two different areas in the Austin Chalk producing trend. Pronounced curvature between the micro-fracture flow region and the matrix flow region results in a qualitative estimate in the difference in the permeabilities between the two flow regimes.

Future Efforts - Work is continuing to relate the Austin Chalk decline curves to total performance curves and to illustrate the ability of decline curves to furnish much the same information which may be obtained from pressure buildup data.

3.2 - Development of a New Enhanced Oil Recovery Process

The Water Imbibition Process - Dr. Perez and Dr. Poston

Brownscombe and Dyes[18] suggested that imbibition flooding could contribute to oil production from the Spraberry trend of West Texas in 1952 . This study established the following conditions for applying a successful imbibition flood: (1) the rock should be preferentially water-wet; (2) the rock surface exposed to imbibition should be as large as possible; and (3) a high oil saturation would greatly benefit the recovery process.

A typical imbibition curve is shown in Fig. 24. Note, most of the recovery is achieved in a rather short length of time. This is a little understood fact in imbibition waterflooding.

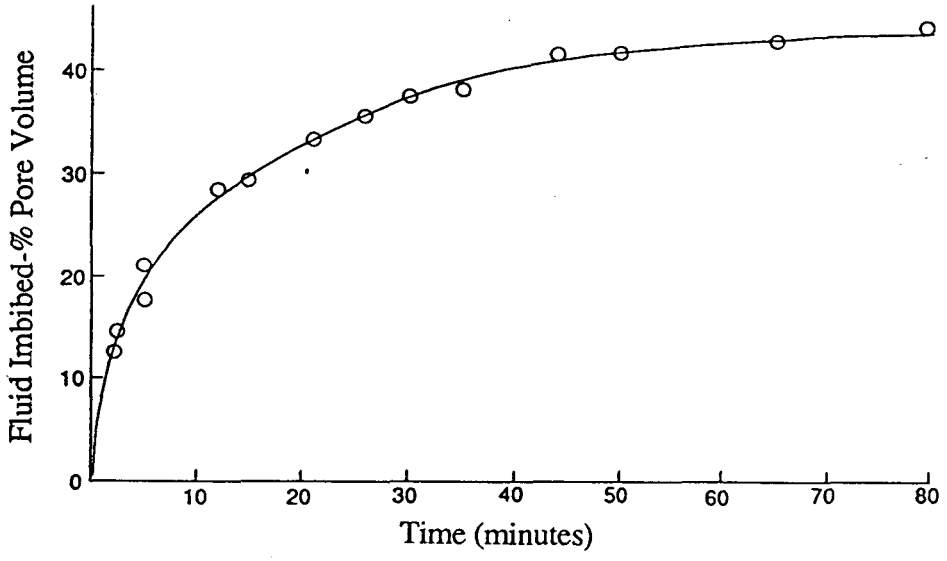

Fig 24 - A Typical Production Curve Resulting from the Imbibition Displacement

Graham and Richardson[19] also derived an equation that describes the imbibition process and defined a reservoir scaling term:

$$\sqrt{\frac{k}{\phi}}\,\frac{\sigma f(\theta)}{\mu_w}$$

This term reveals several facts:

- The oil production rate varies directly with the oil-water interfacial tension.
- The oil production rate is dependent upon the contact angle.
- The rate of imbibition is a function of the viscosity of oil and water.
- The rate of imbibition is a complicated function of the relative permeability and capillary pressure characteristics of the porous medium.

Graham and Richardson also reported that the initial rate of imbibition and the fraction of oil recovered were independent of the sample length and the presence of free gas decreased the rate of water imbibition.

Mattax and Kyte established the basis to scale laboratory results to actual reservoir conditions[20]. The scaling conditions were outlined as follows:

- The shape of the model must be identical to that of the reservoir matrix block.
- The reservoir water-to-oil viscosity ratio must be duplicated in the laboratory tests.
- Initial fluid distributions in the reservoir matrix block and the pattern of water movement in the surrounding fractures must be duplicated in the laboratory tests.
- The relative permeability functions must be the same of the matrix block and the laboratory model.
- The capillary pressure functions for the matrix block and the laboratory model must be directly proportional.

Saturations in the laboratory model will be the same as those in the reservoir matrix block at corresponding times when these conditions are satisfied. One can see that it is essentially impractical to relate laboratory to reservoir conditions and scales if we use current technology. We shall see in later discussions that the use of modern day imaging methods permits us to obtain a much better picture of the imbibition process.

The Enhanced Oil Recovery Concept - Conventional secondary methods cannot be economically applied to fractured reservoirs because injected fluids channel though and only displace the oil located in the fractures. The oil trapped in the matrix blocks is by passed by the injected fluids. Water imbibition is a spontaneous mechanism that would cause water located in the fracture system to be naturally drawn into the matrix block. The process exchanges oil inside the rock matrix for surrounding water filling the fractures. However, this process is very time dependent.

The proposed solution is to use carbonated brine in place of unadulterated water during the imbibition process. The inclusion of CO_2 into the imbibed water will improve the oil recovery efficiency and production rate. The aim of the experimental effort is to blend the CO_2 enhanced recovery characteristics with spontaneous water imbibition method to develop a new recovery oil technique applicable to low matrix permeability, fractured reservoirs.

CO_2 Enhancing Qualities - CO_2 beneficially affects various reservoir properties which result in enhancing oil recovery and recovery rate. The significant interactions of CO_2 with oil, rock, and brine to increase oil recovery by the proposed process are:

- Swelling of Oil - CO_2 is highly soluble in hydrocarbon oils. This swelling effect decreases the volume of residual oil left in the reservoir after flooding.
- Viscosity Reduction - A large reduction in the viscosity occurs when CO_2 is dissolved into a crude oil. This reduction can yield viscosities one-tenth to one-hundredth of the original viscosity.
- Induced Solution Gas Drive - CO_2 evolves from liquid form and acts as an additional reservoir energy when the internal pressure is permitted to decline below the bubble point after the termination of the imbibition phase of a flood. This mechanism of blowdown recovery is similar to solution gas drive during the normal production depletion of an oil field.
- Increased Injectivity - CO_2-water mixtures are slightly acidic and will react with a carbonate rock. Carbonic acid stabilizes clays in shales due to a reduction in pH and injectivity is improved by partially dissolving the reservoir rock.
- Interfacial Tension - A reduction in the interfacial tension between water and oil leads to better mobilization efficiency.

Oil distribution inside carbonated rock samples, and the effects of introducing CO_2 into the imbibed water were studied using conventional laboratory displacement tests, Magnetic Resonance Imaging, *MRI*, Computer Tomography, *CT* analysis methods. The results of each of these different core-fluid interaction studies will be discussed in turn. It must be stated that the results of the imaging work proved to be superior to the laboratory tests. *CT* and *MRI* imaging studies permit cross sectional and longitudinal oil saturation profiles to be measured and recorded as a function of time. The utility of these methods was such, that conventional laboratory displacement studies were dropped from the 3rd year agenda.

Core Sample Preparation - All rock and reference samples used to study imbibition processes were drilled from the same piece of rock to assure similar characteristics. Carbonate as well as quartz sandstones were used in the laboratory experiments while limestone and dolomite cores were used in the imaging studies.

Carbonated water was formed by dissolving CO_2 in brine at some elevated pressure, usually 500 or 1,000 psi. Different concentrations of carbonated brine solutions were achieved by dissolving CO_2 in the brine at different pressures. The CO_2 solubility data of Dodds et al.[22,23] were used in these estimations.

The sequence of laboratory work in the first phase was to prepare, extract, and dry the cores and then determine their basic rock properties. The cores were set in a core holder and flooded to a residual oil saturation.

The flood brine was distilled water mixed with 10,000 ppm $NaCl$. This salt concentration was chosen to be sufficiently high to reduce any possibility of clay interaction and sufficiently low to allow adequate CO_2 solubility. The carbonated brine was usually 1% by wt CO_2 gas dissolved into the brine at standard conditions. Kerosene oil was used to conduct all the experiments. A high pressure core holder was set inside an oven to conduct the laboratory displacement tests. The core holder has dual fluid taps 3/4 inch apart at located at the inlet face of the core. The imbibing fluid is introduced through the lower inlet tap at a very slow rate. The brine sweeps across the core face to be produced through the upper tap. Oil expelled by the imbibition process is produced along with the circulated fluid. A back pressure regulator was used to maintain a 2,000 psi system pressure.

Laboratory Displacement Studies - Both limestone and sandstone core samples were studied. Sandstone permeability ranged from 107 to 389 md while the porosity averaged 20%. The permeability of the limestone cores averaged 9 md and the average porosity was 24%. There was little increase in recovery and insitu permeability in the sandstone cores subjected to both the normal and carbonated water imbibition process. The negligible effect on recovery from the sandstone cores could be caused by their very high permeability. More work should be conducted in this area.

The limestone cores showed increase in recovery and recovery rate when imbibed by carbonated brine. Fig. 25 represents the results of the imbibition experiments conducted on an 8.6 md limestone core. Imbibition displacement by the carbonated water method increased recovery by 26 % and permeability was increased to 10.3 md when compared to the normal water imbibition method. The vertical dotted line at the end of the carbonated brine curve represents an extra 5 % $OOIP$ recovery induced by blowdown effect when pressure was reduced in the imbibition cell to below the bubble point pressure of the carbonated water.

One of the dominant factors causing a recovery increase when carbonated water was used as the imbibing medium was the reduction in interfacial tension. This effect was clearly visible in the glass imbibition cell when experiments were conducted at room temperature and pressure. The number and size of the oil droplets sticking to the core face was found to be much greater in the case of unadulterated brine as compared to carbonated brine.

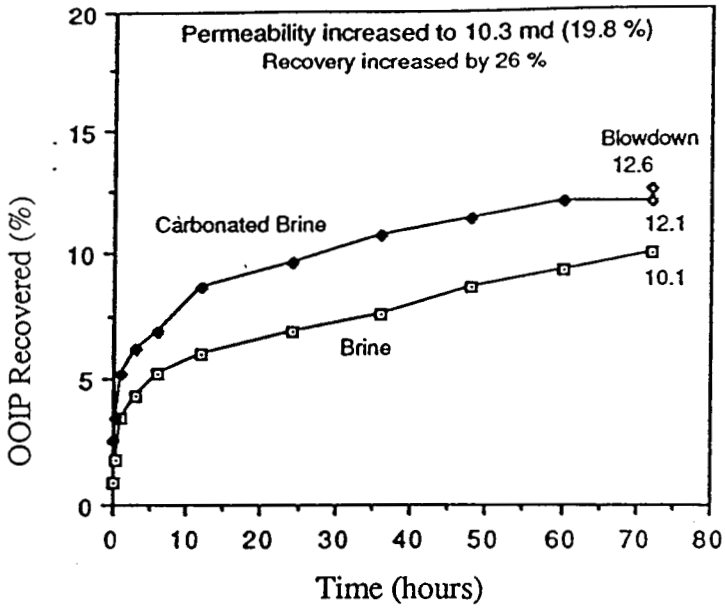

Fig. 25 - Comparing Recoveries from a Limestone Core - Constant Temperature

Fig. 26 compares the results of the imbibition experiments conducted for 48 hours at 70 °F and 110 °F temperature and 500 psi pressure using 4 % by weight carbonated brine. A 4% by wt carbonated brine is equivalent to 130 cu ft of CO_2 gas dissolved in one barrel of 10,000 ppm brine at standard conditions.

An additional 34.2 % of *OOIP* was recovered at a 110 °F when compared with the recovery at 70 °F. The initiation of a reservoir blow down process yielded 12.7 % of *OOIP* at 70 °F and 16.6 % of *OOIP* at 110 °F. As would be expected, the solution gas-drive effect is more pronounced at higher temperatures.

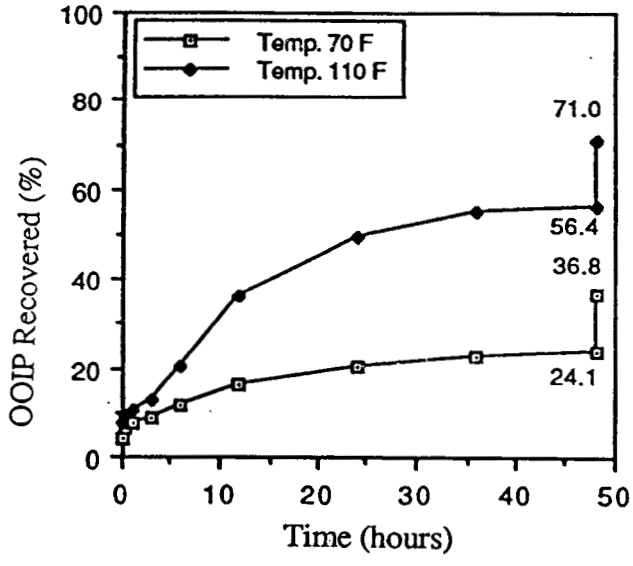

Fig. 26 - Illustrating the Effect of Temperature on Oil Recovery from a Limestone Core

Fig. 27 illustrates the effect of CO_2 concentration in the imbibed water on ultimate recovery and recovery rate. An increase of 2.25 % to 4 % by wt in concentration of dissolved CO_2 in brine yielded an additional recovery of 50.9 % of *OOIP*. The blow-down effect after imbibing with the low CO_2 concentration brine resulted in a 6 % of *OOIP* increase in recovery, while the high CO_2 concentration brine resulted in an additional recovery of 14.6 % of *OOIP*. These experiments were conducted at 500 psi imbibition pressure and 110 °F temperature.

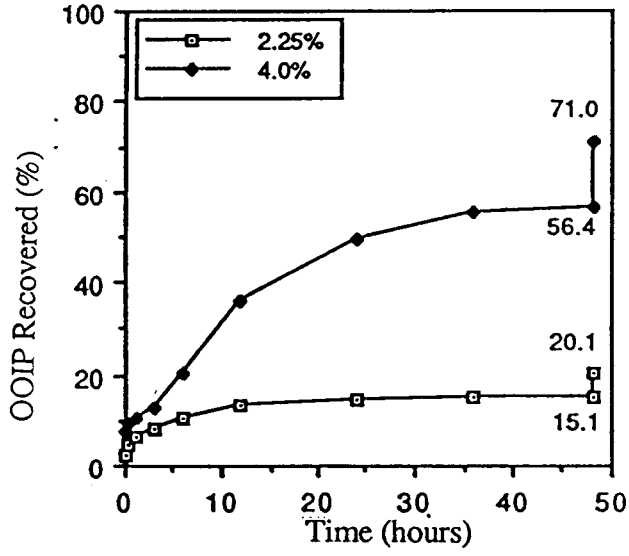

Fig. 27 - The Effect of CO_2 Concentration on Oil Recovery

Preliminary microscopic studies on the 9 md limestone indicated no discernable effect of matrix dissolution due to acidic nature of the carbonated brine. More work is to be conducted in this area.

MRI Studies - Proton profile images were to used to map any oil saturation changes inside the rock samples. Deuterium Oxide, D_2O was used in place of water to insure only oil protons were observed. Two dimensional images were recorded. Longitudinal images of the sample were primarily taken to observe oil saturation changes and movement along the main axis of the sample. A typical proton profile image is shown in Fig. 28. The number of protons or the oil saturation increases upward on the "y" axis. The figure is illustrative of a core sample flooded to a residual water saturation and ready for a water imbibition displacement test. Water was introduced into the small reservoir at the face of the core from a lower lying tap. The oil seen in the spike located at the core face will be displaced through the upper tap. Imbibition of water into the core will commence at this time. A

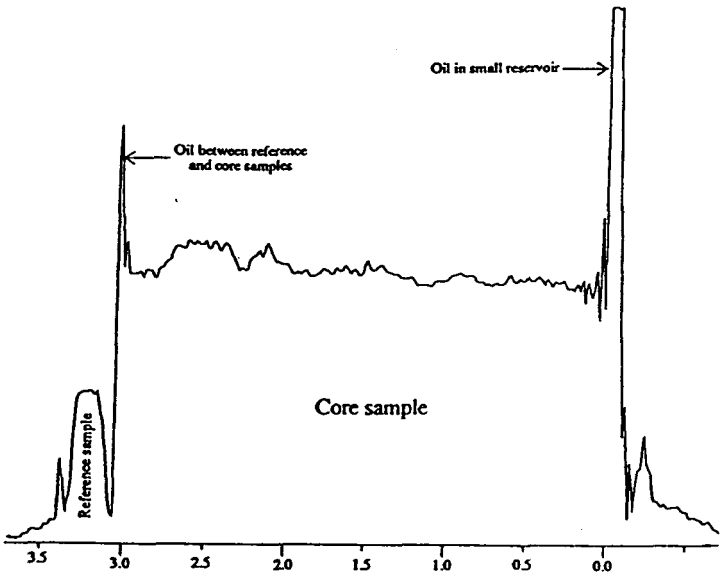

Fig. 28 - A Typical Proton Profile. Reference and Core Samples are Identified

reference sample is included in the profile to allow saturations measured at different time intervals to be related to each other, i.e., to be normalized.

The integral of the signal from the reference sample was used to normalize all the experimental data. The subtraction of profiles permits the changes in oil saturation as a function of time to be quantified. A typical reconstructed set of oil saturation profiles observed during a normal brine imbibition flood is seen in Fig. 29.

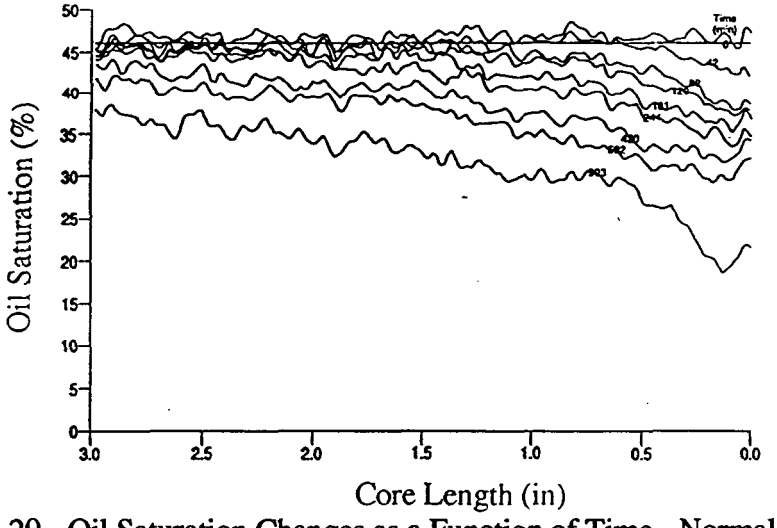

Fig. 29 - Oil Saturation Changes as a Function of Time - Normal Brine Imbibition

Notice, the oil saturation profiles decrease in an orderly manner from 0 to 903 minutes. The profiles appear to consist of a straight line trend from the core face to 0.5 in, with a straight line of lesser slope extending from 0.5 to 3 in. The high water saturation close to the core face may be an end effects problem. More work should be done to quantify this phenomenon. It is evident that the produced oil originates over the complete length of the sample.

Fig. 30 shows a cumulative oil production curve obtained by integrating the areas of each of the normalized curves to determine displaced oil volumes. This method permits the amount of oil moved inside the rock sample to be calculated without the need for accounting for the volume of oil adhering to the rock surface.

An artificial gas drive was induced after the major effects of water imbibition displacement were dissipated for CO_2-enriched water imbibition displacement experiment. The pressure was dropped below the bubble point after the oil production rate became insignificant. The pressure decrease permitted the dissolved CO_2 to evolve from liquid form. An artificial solution gas drive was created inside the sample. This localized gas drive expels liquids out of the rock. A substantial decrease in oil saturation is observed when this phenomena is induced. Fig. 31 presents a before and after profile resulting when such a process is induced in a core sample.

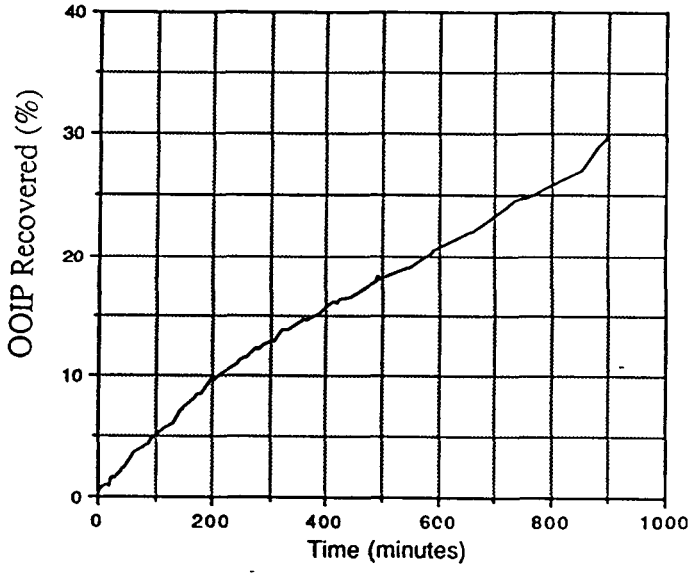

Fig. 30 - Cumulative Oil Production During Imbibition Displacement of Pure Water

Subtraction of the profiles before and after the pressure decrease presents a better description of the fluids movement inside the sample, see Fig. 32. Oil was forced out of the rock, but at the same time, a smaller volume of oil was forced inside the sample. On

the other hand, a drop of the system pressure caused no effect when unadultered water was being used.

Oil saturation profiles do not exhibit the straight line trend shown for the case of pure water. A more accentuated decrease in oil saturation closer to the imbibing rock face was observed for the CO_2 cases. Fig. 32 illustrates this dual slope nature. It is important to point out the dramatic decrease in oil saturation close to the imbibing face after the gas expansion. The drastic decrease in oil saturation in only one region of the sample reveals that the carbonated water was not reaching the full length of the rock. The CO_2 is confined close to the core face. CO_2 entrained in the imbibing water diffuses to the oil phase which is counter currently migrating to the core face is the cause for this phenomena. This is an obvious limiting factor for this process as well as with all types of CO_2 enhanced recovery processes. To our knowledge this is the first time this phenomena has been noted.

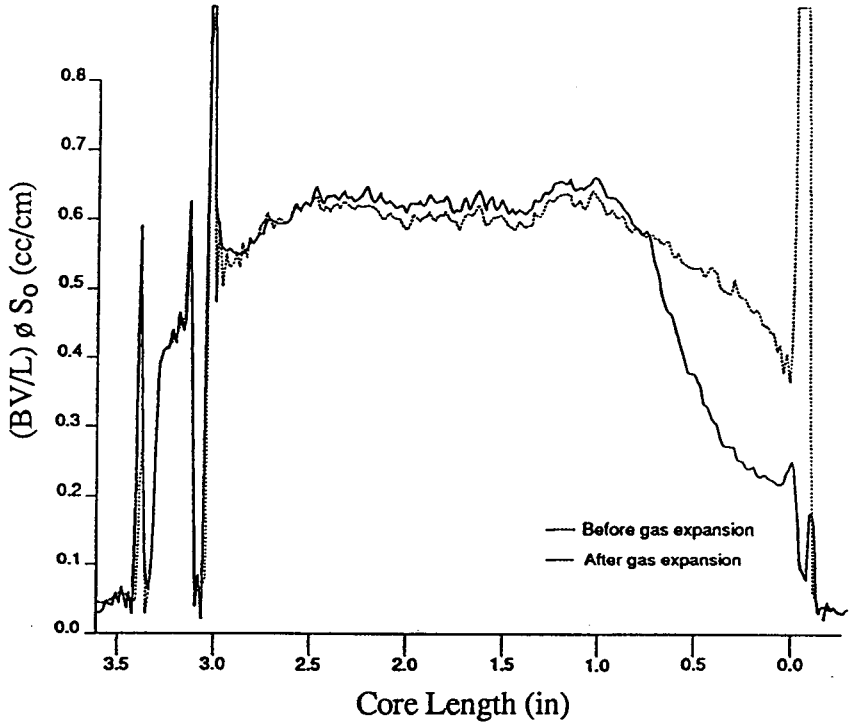

Fig. 31 Oil Saturation Profile Illustrating the Effect of the Induced Solution Gas Drive

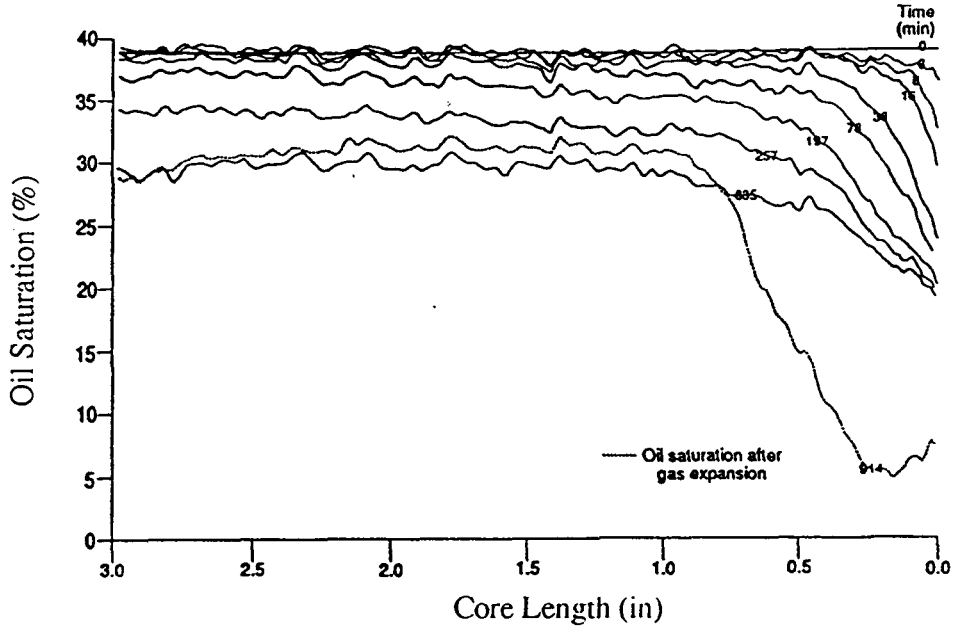

Fig. 32 - Illustrating the Combined Effect of a Carbonated Water - Induced Solution Gas Drive Depletion Study

Fig. 33 is the result of integrating the oil saturation profiles shown in Fig. 32. It is evident the cumulative production curve was modified by the expansion of dissolved CO_2. Note, an exponential curve is evident during the first part of the displacement process.

CO_2-enriched water imbibition and the localized gas drive created by the gas expansion were combined into a cyclic sequence to study the effect of repeated treatments on ultimate recovery and rate of recovery. This combination of imbibition and pressure pulsing produced a cyclic imbibition type of production. The new method combines several interesting advantages for increasing oil recovery. The sequence of events are as follows:

- The imbibition phenomena is used to carry the dissolved CO_2 into the core.
- The ability of CO_2 to preferentially diffuse from the water to the oil is used.
- The newly arrived CO_2 beneficially affects the oil properties which in turn increases the migrating abilities of the oil.
- A localized gas drive is created when the pore pressure is dropped below the bubble point pressure.
- A cyclic process keeps reintroducing the carbonated water into the reservoir, which to a great extent nullifies the "thieving" problem of the imbibed CO_2 diffusing to the produced oil.

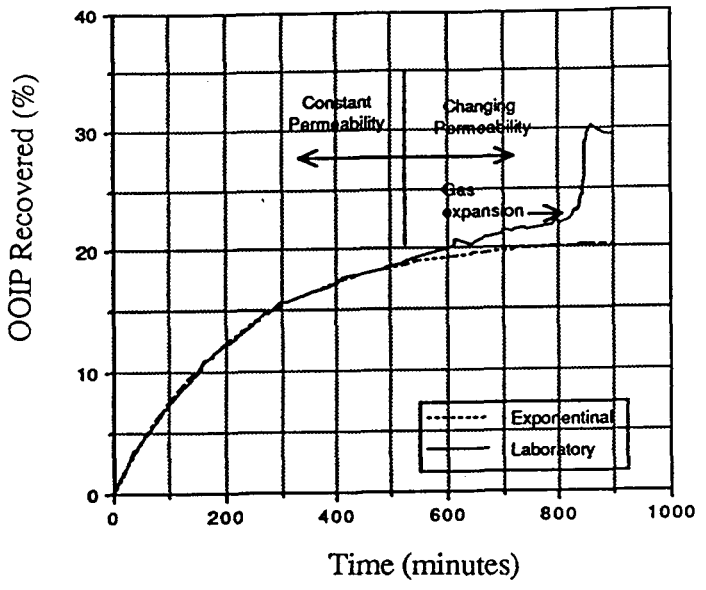

Fig. 33 - Cumulative Oil Production Obtained by Imbibition of Carbonated Water

Fig. 34 compares oil saturation profiles at initial conditions and after 3 carbonated water imbibition-induced solution gas drive cycles. Note, the ability of the cyclic process to move the region of low oil saturation further out into the core.

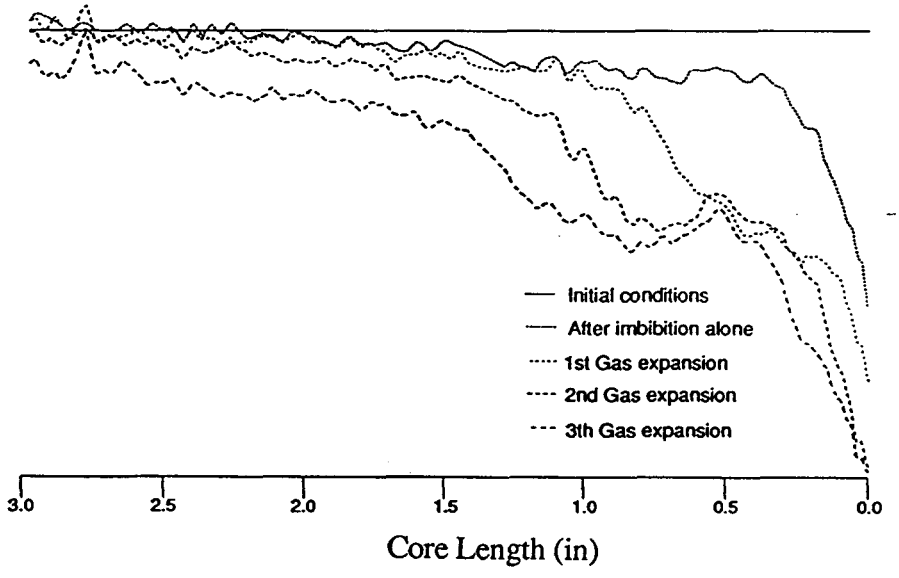

Fig. 34 - Profiles Showing the Effect of the Cyclic Process

Visualization of Fractures in Austin Chalk - The mapping of microfractures using a non-destructive technique is a unique application of *CT* imaging. An attempt is being made to determine average fracture length, distribution of microfractures, and the relationship between interconnected and discontinuous microfractures from cores obtained from an Austin Chalk horizontal well.

Cores are prepared for scanning by placing the cores into a low vacuum core holder. The core is then subjected to evacuation at ultra-low vacuum pressures for a period of up to one week. Scanning of the subject is then initiated. Xenon gas is introduced into the core holder at low pressure (15 psig) after the initial scan of the evacuated core. The core is then rescanned using the same z axis locations.

Xenon gas has an atomic weight of 131 and the atomic weight of air is 29. Because of the difference in weights, xenon has an x-ray attenuation approximately four and a half times that of air. The xenon gas collects in the open pore spaces, i.e., fracture and vugs, and enhances the resulting *CT* images. The presence of stress relief perimeter fractures, micro-fractures and vugs were easily discernable. Example figures are not included because definition of black and white photos is limited. The actual *CT* images are projected on a color scale to emphasize these discontinuities.

Conclusions - Laboratory and imaging studies have proven the theoretical efficacy of replacing normal water with carbonated water to increase oil recovery and rate of recovery with the imbibition displacement method. *MRI* proton profiles proved that CO_2 dissolved in the water being imbibed into the rock sample did not reach the full length of the rock sample. The evidence suggests that CO_2 diffuses to the counter current flowing oil which in turn is expelled at the imbibing face.

A combination of CO_2 - enriched water imbibition and pressure depletion created a cyclic type of recovery. This method combined the beneficiating effects of CO_2 at early times, and the increase in oil production due to the localized gas drive observed after pressure depletion. The time needed to recover similar amounts of oil was reduced to nearly one third of the time required when unadulterated water imbibition was applied. This method exhibited the highest rate of recovery.

Micro-fractures present in Austin Chalk core samples were easily identified and mapped with *CT* imaging.

Transfer of Technology -The following is a listing of the presentations and publications pertaining to these subjects which were presented during the year.

1. Grape, S.G., "Imbibition Flooding With CO_2-Enriched Water": A M.S. Thesis in Petroleum Engineering, Texas A & M University. (Aug. 1990)
2. Poston, S. W., Perez, J. M., and Halimi, H., "Preliminary Studies - Using MRI Imaging Techniques to Study Water Imbibition Flooding," Presented at the 6th Wyoming Enhanced Oil Recovery Symposium, May 3-4, 1990, Casper, WY.
3. Halimi, H., Capp, K., and Poston, S. W., "Using a Personal Computer to Process MRI Data," SPE 20353. Presented at the 1990 SPE Petroleum Computer Conference held June 25-26, 1990 in Denver, CO.
4. Grape, S.G., Poston, S.W., and Osoba, J. A., "Imbibition Flooding with CO2-Enriched Water," SCA #9018. Presented at the Fourth Annual Society of Core Analysts Technical Conference, August 15-16, 1990, Dallas, TX.

Mathematical Modeling of The Carbonated Water Imbibition Process - Dr. Wu

The purpose of this research is to develop a mathematical model to describe the imbibition recovery process of a carbonated waterflood in naturally-fractured porous media. The mathematical modeling effort is divided into two parts. The first part deals with the development of analytical models for a parametric study of laboratory imbibition waterflood performance. The second part deals with the development of a compositional numerical simulator for field scale, carbonated-water imbibition flood in fractured reservoirs.

Many analytical and numerical mathematical models for fluid flow in fractured reservoirs are presented in the literature. de Swann[23] presented an analytical model describing the imbibition of water displacing oil process in a fracture surrounded by matrix blocks. The fractional flow of water is equal to the water saturation at the same spatial point was assumed in order to linearize the equation. Kazemi *et al*[24] improved the analytical solution technique over that presented by de Swaan and attempted a numerical solution as well. A good match was obtained by both solution methods. A new iterative semi-analytical technique was developed to solve the aforementioned nonlinear integro-differential equation. The solution method was improved using the Stehfest algorithm to invert from the Laplace domain to real domain. The effect of viscosity ratio was significant in determining the flood performance.

The limitations associated with the analytical modeling and the complex oil recovery mechanisms involved in carbonated waterflooding in a dual porosity system require a numerical model to effectively describe the oil recovery mechanism/s. The first compositional simulator was presented by Peng *et al*[25]. The dual-porosity approach was used. The implicit in pressure and explicit in saturation, *IMPES* method was applied.

Analytical Modeling - The following differential-integral equation developed by de Swaan[23] is solved to analyze laboratory imbibition waterflood performance:

$$-u_f \frac{\partial f_{wf}}{\partial x} = \frac{\partial S_{wf}}{\partial t} + \frac{\lambda R_\infty}{\phi_f} \int_0^t e^{-\lambda(t-\tau)} \frac{\partial S_{wf}}{\partial \tau} d\tau \qquad (1)$$

The following differential-integral equation which is similar to that proposed by Davis and Hill[26] was developed for the matrix system when the proper boundary conditions were imposed

$$0 = \frac{\partial S_{wm}}{\partial t} - \frac{\lambda R_\infty}{\phi_m} \int_0^t e^{-\lambda(t-\tau)} \frac{\partial S_{wf}}{\partial \tau} d\tau \qquad (2)$$

where the initial condition is, $S_{wm}(x,o) = S_{wmirr}$

It is difficult to obtain the solution to the de Swaan equation. An analytical approach for a non-unity mobility ratio is out of question, while a numerical method is plagued by numerical instability. Both de Swaan and Kazemi, *et al* linearized the differential-integral equation by assuming the water fractional flow in the fracture is equal to the corresponding water saturation in the fracture. Davis and Hill linearized the equation by assuming the water fractional flow to be equal to the ratio of water saturation and the water-oil viscosity ratio.

An attempt was made to solve the nonlinear integro-differential equation by an iterative semi-analytical technique. Therefore, these simplifying assumptions were not required. The fractional flow gradient in Eq. 1 is factored as follows:

$$-u_f \left(\frac{df_{wf}}{dS_{wf}}\right) \frac{\partial S_{wf}}{\partial x} = \frac{\partial S_{wf}}{\partial t} + \frac{\lambda R_\infty}{\phi_f} \int_0^t e^{-\lambda(t-\tau)} \frac{\partial S_{wf}}{\partial \tau} d\tau \qquad (3)$$

The coefficient of the saturation gradient term in Eq. 3 is calculated using the saturation at the beginning of the time step and the solution to the equation at a specified location is obtained by Laplace transformation. In Laplace domain, Eq. 3 is transformed as

$$-uf_w' \frac{d\widetilde{S_{wf}}}{dx} = s\left(1 + \frac{\alpha}{s+\lambda}\right)\widetilde{S_{wf}} \qquad (4)$$

Solving Eq. 4 in the Laplace domain with the proper boundary condition results in:

$$\widetilde{S_{wf}} = e^{-\alpha s}\left(\frac{1}{s}e^{\frac{\alpha\lambda s}{s+\lambda}}\right) \qquad (5)$$

The Laplace transform of the saturation is inverted to obtain the real time saturation by using the Stehfest algorithm. For each time step the procedure is iterated using the updated saturation until the saturation difference between iterations converges to within a given tolerance.

Solution to the equation provides a saturation profile in the fracture as a function of time. The saturation history at the outlet is used to calculate the fractional flow of oil and water, thereby, the water cut and oil production rate. Once the saturation in the fracture is calculated, the water saturation in the matrix system can be calculated.

The nonlinear solution technique was used to analyze the Kazemi *et al*[24] laboratory imbibition waterflood data. The calculation showed that a good fit was obtained when the imbibition rate is constant and $\lambda = 120$.

Fig. 35 shows the water saturation distribution curves in the fracture at increasing time steps.

A hypothetical field case published by Kazemi et. al was also analyzed to show the applicability of the semi-analytical model. The results of the newly developed method were found to agree with the Kazemi et al approach.

Results of this study indicated that the viscosity ratio is limited to the range between 0.25 and 2.0. Results of initial sensitivity study also indicated that the results are very sensitive to the variation in injection rate. Further investigation on the limitations of this approach are in order. A compositional numerical modelling will be needed to provide reasonable mathematical solutions because of these limitations.

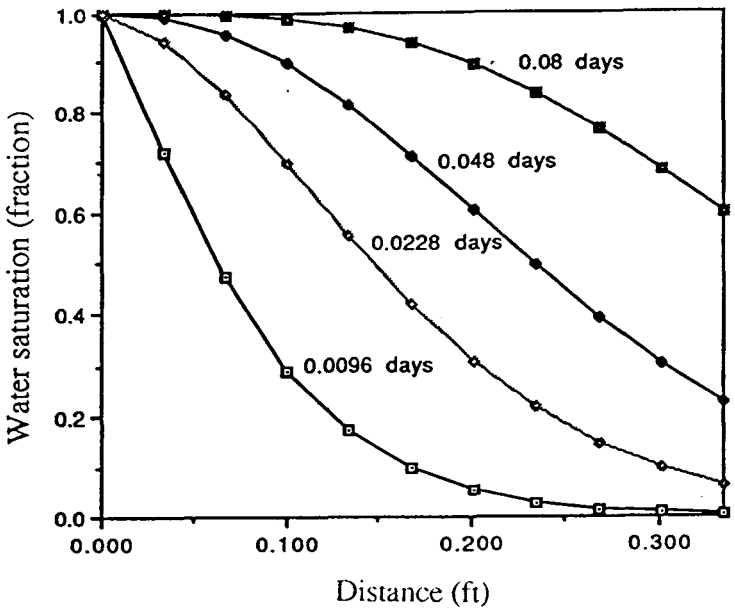

Fig. 35 - Calculated Fracture Water Saturation Profile

Numerical Modeling - The limitations associated with the analytical modeling of a CO_2-enriched waterflood in a naturally-fractured reservoir requires a numerical compositional simulation model. The modification of our existing compositional single-porosity simulator to a dual-porosity compositional simulator has been completed. Testing, debugging and validation of the newly developed model are underway.

A simplified representation of a naturally fractured porous medium is shown in Fig. 36. The matrix system and fracture system are superimposed for the naturally fractured porous medium with their average rock and fluid properties.

The differential material-balance equations for a component for matrix and fracture fluid transfer were written. Mass-balance finite difference equations for each phase were developed for the fracture and matrix systems. The total mass balance between the neighboring fracture grid blocks and fracture/matrix fluid transfer can be expressed for the fracture grid block (i,j,k). The pressure difference between two time levels is determined by differentiating the residual equations for the fracture and matrix systems with respect to each grid block after converting the pressures of water and gas to the oil pressure using the appropriate capillary pressure values in a Jacobian matrix.

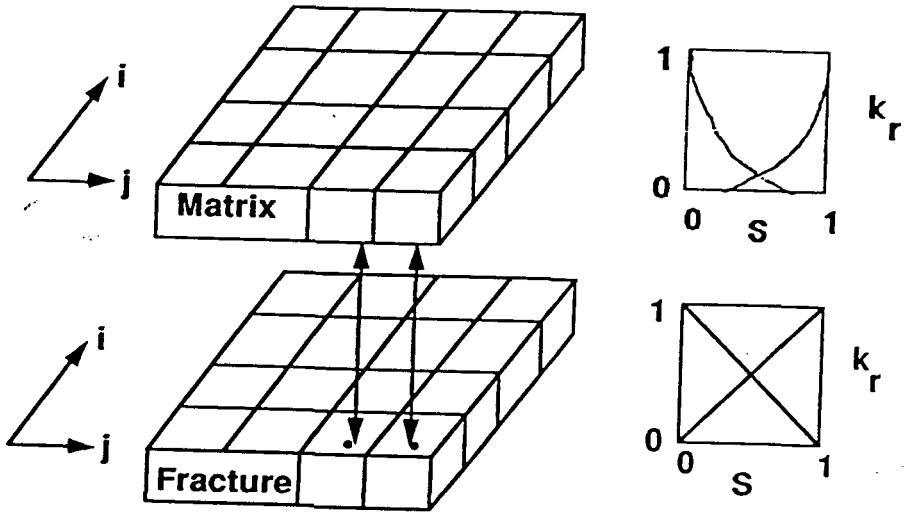

Fig. 36 - An Idealized Model of Naturally Fractured Porous Medium

The basic information for a hypothetical test case are presented in the following table. All relevant data are taken from SPE Test Case Number 5[27] except for the relative permeability data for the fracture system which is assumed to be a function of the water saturation, ie, $K_{rw} = S_w$. A single block tank type model was used. The pressure vs time profile for each system is presented in Fig. 37.

Hypothetical Field Case Data for Numerical Simulation

Length - X direction = 500 ft, Y direction = 500 ft, Z direction) = 20 ft
Initial water saturation = 0.2, Initial gas saturation = 0.0
Matrix System, $\phi = 0.3$, k = 500 md
Fracture System, $\phi = 0.05$, k = 5,000 md

The resulting pressure profiles from the simulation run is shown below. Note the dramatic difference in matrix and fracture presses at mid to late times.

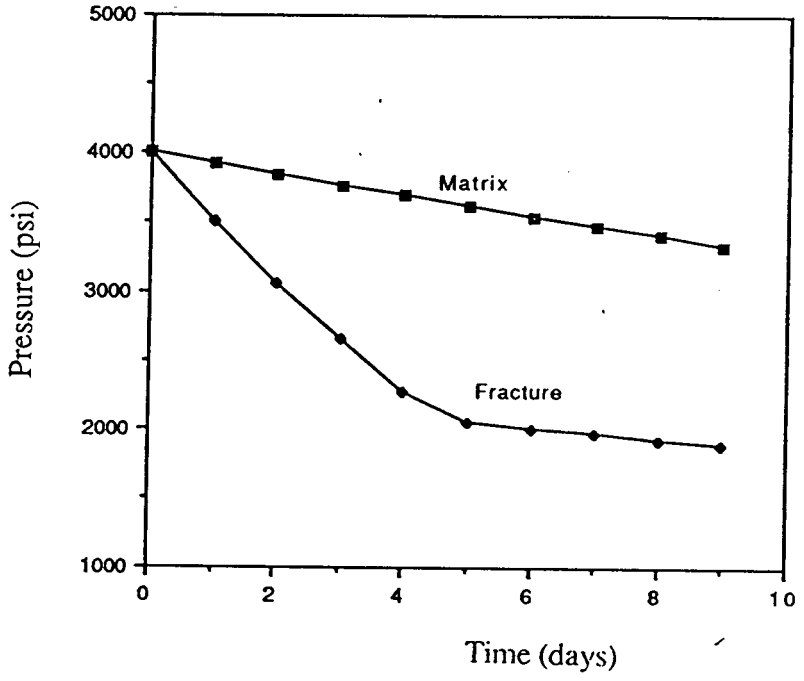

Fig. 37 - Pressure Profiles in the Matrix and Fracture Systems

3.3 - Field Test and Transfer of Technology

Edco Producing Company has expressed an interest in conducting a trial, carbonated water frac treatment on their Wilson-Dunn Unit No. 1 well. The well has been scheduled for treatment in the 3rd quarter of 1992

The following characteristics of the fractured reservoir system and fluid properties were derived from the previously discussed studies:

- Outcrop studies indicate that the following geometry could represent an Austin Chalk reservoir: Matrix blocks of about 4 X 4 X 4 ft and a system of macro-fractures 0.8 mm wide. The micro-fractures are 0.1 mm wide
- The producing interval was assumed to be 80 ft thick.
- The movable oil saturation in the matrix blocks after primary recovery is 45%. Laboratory experiments have shown an additional oil recovery due to carbonated water imbibition of 15% of *OOIP*.
- A gaseous phase is present in the fracture system. Dissolved gas drive is assumed to be the primary production mechanism.
- The average depth of the reservoir, in the area of interest, is 5,500 ft with a *BHT* of 170 ^{o}F.
- Representative reservoir matrix rock, fluid characteristics, and laboratory rock and fluid properties are shown in the following table. Laboratory characteristics were needed to scale the obtained results to reservoir scale.

Several considerations have to be done in order to duplicate the beneficial effects of a carbonated water imbibition flooding seen in repeated laboratory experiments using Austin Chalk crude.

Water imbibition is directly proportional to the contact area between the rock and water. The surface area contacted by the carbonated water must be as large as possible. This consideration suggests that the largest possible volume of carbonated water be injected.

Laboratory experiments have shown that oil recovery is proportional to the amount of CO_2 dissolved into the imbibed water. Fig. 38 shows the solubility of CO_2 in water is a direct function of pressure and is greatest at low pressures. At high pressure values the solubility becomes approximately a linear function of pressure. Carbon dioxide solubility in water is also a function of temperature and salinity. Increases in temperature will

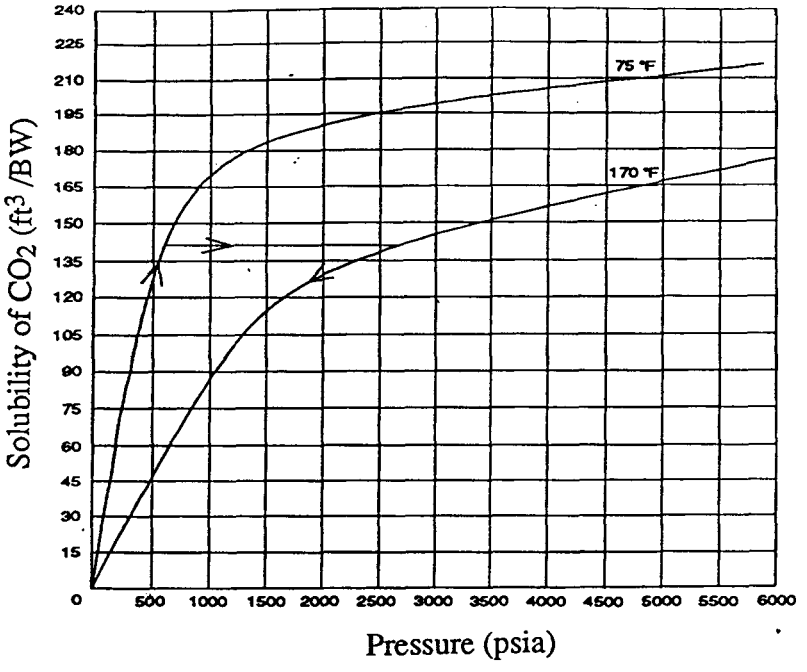

Fig. 38 - Solubility of Carbon Dioxide in Water

decrease the solubility. The amount of CO_2 dissolved in water will remain constant from a surface mixing pressure of 650 psi at surface temperature, to a bottom hole pressure and temperature of 3000 psi and 170 °F respectively. The ability to increase and maintain an elevated reservoir pressure is a key factor in determining the successful outcome of the process.

Oil recovery due to carbonated water imbibition displacement-oil recovery would be generated from two different sources: (1) Oil being displaced by the imbibed water and produced from the matrix itself, and (2) Oil removed from the fracture system due to the localized gas drive installed by reducing the system pressure below the mixing pressure. Additionally, a gaseous phase originating in the matrix and migrating to the fractures would remove small droplets adhering to the surface of the rock.

Oil production due to carbonated water imbibition could be calculated scaling laboratory results to field applications. Laboratory experiments have shown a cumulative oil production of about 15% of *OOIP*. The observed laboratory recovery translates to about 630 stb/acre from the matrix.

CO_2 evolves to its gaseous state when the system pressure is decreased below the bubble point. This localized gas drive forces some oil out of the rock matrix. In addition, the gas production from inside of the rock matrix will initiate production of crude adhering to the rock surface. Laboratory experiments have shown a decrease in the amount of crude

oil adhering to the rock surface from 6.5 to 3.9 cm^3 of crude / 100 cm^2 of imbibing area. The amount of adhering oil translates to a total of 1,062 Bbl of crude/acre of reservoir. The rock and fluid properties for both the laboratory and field test conditions are listed in the following table.

	k_{matrix} (md)	ϕ_{matrix} (%)	σ (dyne/cm)	Imb. depth (in)
Reservoir	0.002	3	15	3
Laboratory	10	26	33	3

Total oil production - The summation of all of these incremental effects yields a total oil production of 1,692 Bbl/acre. The following table illustrates this summation.

Predicted Recovery and Rate of Recovery

			Producing Characteristics			
Interval Thickness (ft)	S_o (%)	$S_{o(movable)}$ (%)	Imbibition Recovery (Bbl/acre)	Fracture Face Cleaning (Bbl/acre)	Total Recovery (Bbl/acre)	Required Time (days)
80	45	15	630	1062	1692	106

The scaling equation developed by Mattax and Kyte[20] was used to scale model time to reservoir time:

$$\left[t\sqrt{\frac{k}{\phi}\frac{\sigma}{\mu_w L^2}}\right]_{model} = \left[t\sqrt{\frac{k}{\phi}\frac{\sigma}{\mu_w L^2}}\right]_{reservoir}$$

An equivalent reservoir time to model time is obtained when the necessary parameters are input into this equation:

$$t_{reservoir} = t_{model} * 52.84$$

This is the time required to reach equivalent oil saturation conditions. The observed t_{model} to achieve maximum oil recovery has been about 48 hrs. Therefore, the time needed to achieve maximum oil recovery $t_{reservoir}$ = 106 days.

4.0 Conclusions

Geological Studies - Detailed maps of the fracture traces on bedding planes in the mapped Austin Chalk outcrops were prepared. The maps showed the organized trends of the fracture development and hierarchical nature within the complete fracture system. These efforts were very useful to the development of a representative set of production decline type curves particular to a dual fracture-matrix flow system. Work for the next year will translate these efforts to subsurface interpretation.

Geophysical Studies - VSP data has been obtained for estimating fracture orientations from shear-wave splitting. Several programs had to be written to facilitate analysis of the data. Good progress had been achieved in fracture imaging.

Task 2 - Relating Recovery to Well-Log Signatures

Geological Studies - Well-log response in Austin Chalk wells has been shown to be a reliable indicator of organic maturity. Work conducted during the previous year has been to digitize well logs in order to calculate average resistivity of producing zones and to correlate resistivity with production decline characteristics. These studies are still preliminary in nature, and it is still early to derive any significant conclusions.

Petroleum Engineering Studies - Additional production decline data were digitized to provide other interpretation examples for the dual permeability-matrix flow type curves developed during the first year. Darcy's law was modified in an attempt to account for the non-homogeneous internal structure of a fractured medium and the permeability contrast between the fractures and the matrix blocks. Work is continuing on this subject.

Task 3 - Development of the EOR Imbibition Process

Laboratory Displacement Studies - Displacement studies were continued from the efforts of the previous year with the development and fabrication of a high pressure-high temperature core holder. Increased temperature was found to accelerate and increase oil recovery by the carbonated water-imbibition process.

MRI Studies - Image scanning studies have shown the carbonated water imbibition displacement process accelerates and increases recovery of oils which do not have appreciable asphaltenes. Experimental work conducted in a core saturated with an oil containing asphaltenes were halted because of pore blocking by ashphaltene deposition.

A study of recovery by cyclic carbonated water imbibition followed by reducing the pressure below the bubble point of the CO_2-water solution indicated the possibility of a new enhanced recovery method. Additional work is being conducted in this area.

CT Studies - Equipment has been constructed and tested which will allow long term imbibition studies to be conducted on 1 md core sample with the CT scanner.

Extent and arrangement of miro-fractures in Austin Chalk horizontal cores was mapped with CT scanning techniques. The degree of interconnection of the micro-fractures was easily visualized.

Task 4 - Mathematical Modeling - Both the semi-analytical and numerical models for studying the imbibition flooding method have been developed. Model testing is continuing.

Task 5 - Field Tests - Two operators amenable to conducting a carbonated water flood test on an Austin Chalk have been identified. We are still evaluating the ability of their crude to not form asphaltene residue in the presence of CO_2.

The efforts for the second year may be summarized as one of coalescing the initial concepts developed during the initial phase to more in depth analyses.

5.0 - References

1. Hinds, G.S., and Berg, R.R., (1990), "Estimating Organic Maturity from Well Logs, Upper Cretaceous Austin Chalk, Texas Gulf Coast," *Gulf Coast Association of Geological Societies Transactions*, v. 40, p. 295-300.

2. Corbett, Kevin, Friedman, M., and Spang, J., (1987), "Fracture Development and Mechanical Stratigraphy of Austin Chalk, Texas," *Am. Assoc. Petroleum Geol. Bulletin*, v. 71, p. 17-28.

3. Bieniawski, Z.T., (1984), *Rock Mechanics Design in Mining and Tunneling*, A.A. Balkema Publishers, Rotterdam and Boston, 272 p.

4. Grabowski, G.J., Jr., (1984), Generation and Migration of Hydrocarbons in Upper Cretaceous Austin Chalk, South-Central Texas," in J.G. Palacas, editor, Petroleum Geochemistry and Source-Rock Potential of Carbonate Rocks: AAPG Studies in Geology 19, p. 97-115.

5. Hinds, G.S., and Berg, R.R., (1990), "Estimating organic maturity from well logs, Upper Cretaceous Austin Chalk, Texas Gulf Coast," *Gulf Coast Association of Geological Societies Transactions*, v. 40, p. 295-300.

6. Hunt, J.M., and A. P. McNichol, (1984), "The Cretaceous Austin Chalk of South Texas-A Petroleum Source Rock," in J. G. Palacas, editor, Petroleum Geochemistry and Source-Rock Potential of Carbonate Rocks: AAPG Studies in Geology 18, p. 117-125.

7. Barenblatt, G.I. and Zheltov, Yu. P.: "Fundamental Equations of Filtration of Homogeneous Liquids in Fissured Rocks," *Soviet Physics - Doklady* (1960) **5**, 522-25; (English Translated for *Doklady Akademii Nauk SSSR* (1960) **132**(3) 545-48.)

8. Barenblatt, G.I., Zheltov, Iu.P. and Kochina, I.N.: "Basic Concepts in the Theory of Seepage of Homogeneous Liquids in Fissured Rocks (Strata)," **PPM** (1960) **24**(5) 1286-303; (English Translated from *Priklad. Mat. Mekh.* (1960) **24**(5) 852-64; *J. App. Math. and Mech., USSR.*)

9. Warren, J.E. and Root, P.J.: "The Behavior of Naturally Fractured Reservoirs," *SPEJ* (Sept. 1963) 245-55; *Trans.*, AIME, **228.**

10. Wijesinghe, A.M. and Culham, W.E.: "Single-Well Pressure Testing Solutions for Naturally Fractured Reservoirs with Arbitrary Fracture Connectivity," paper SPE 13055 presented at the 1984 Annual Technical Conference and Exhibition, Houston, TX, Sept. 16-19.

11. Chen, H.Y., Poston, S.W. and Raghavan, R.: "The Well Response in a Naturally Fractured Reservoir: Arbitrary Fracture Connectivity and Unsteady Fluid Transfer," paper SPE 20566 presented at the 1990 Annual Technical Conference and Exhibition, New Orleans, LA, Sept. 23-26.

12. Kazemi, H.: "Pressure Transient Analysis of Naturally Fractured Reservoirs with Uniform Fracture Distribution," *SPEJ* (Dec. 1969) 451-58.

13. de Swaan, O.A.: "Analytic Solutions for Determining Naturally Fractured Reservoir Properties by Well Testing," *SPEJ* (June 1976) 117-22, *Trans.*, AIME, **261.**

14. Fetkovich, M.J.: "Decline Curve Analysis Using Type Curves," *Jour. Pet. Tech.* (June 1980) 1065-77.

15. Chen, H.Y.: "Well Behavior in Naturally Fractured Reservoirs," (August 1990) Ph.D. Dissertation, Texas A&M University.

16. Poston, S.W., Chen, H.Y., and Sandford, J.R.: "Fitting Type Curves to Austin Chalk Wells," SPE 21653. Presented at the 1991 Production Operations Symposium, Oklahoma City, OK.

17. Chen, H.Y., Raghavan, R., and Poston, S.W.: "The Well Response in a Naturally Fractured Reservoir: Arbitrary Fracture Connectivity and Unsteady Fluid Transfer," SPE 20566. Presented at the SPE Annual Technical Conference and Exhibition, Sept. 23-26, 1990, New Orleans, LA.

18. Brownscombe, E.R., and Dyes. A.B.: "Water-Imbibition Displacement . . . Can it Release Reluctant Spraberry Oil?," *Oil and Gas J.* (Nov. 17, 1952) 264-65.

19. Graham, J.W., and Richardson, J.G.: "Theory and Application of Imbibition Phenomena in Recovery of Oil," *Trans.*, AIME (1959) 216, 377-381.

20. Mattax, C.C., and Kyte, J.R.: "Imbibition Oil Recovery from Fractured, Water-Drive Reservoirs," *JPT* (June 1962) 177-184.

21. Dodds, W.S., et al.: "CO_2 Solubility in Water," Chem. Eng. Data Series 1, *Gas Jour.*, (Oct. 8, 1962).

22. Dodds, W.S., Stutzman, L.F., and Sollami, B.J.: "Carbon Dioxide Solubility in Water," *J. Ind. and Eng. Chem.* (1956) **1**, 92-95.

23. de Swaan, A.: "Theory of Waterflooding in Fractured Reservoirs," *SPEJ* (April 1978) 117-22.

24. Kazemi, H., Gilman, J.R., and El-Sharkaway, A.M.: "Analytical and Numerical Solution of Oil Recovery from Fractured Reservoirs Using Empirical Transfer Functions," paper SPE 19849 presented at the 1989 SPE Annual Technical Conference and Exhibition, San Antonio, TX, October 8-11.

25. Peng, C.P., Yanosik, J.L. and Stephenson, R.E.: "A Generalized Compositional Model for Naturally Fractured Reservoirs," *SPERE* (May, 1990) 221-226.

26. Davis, G.B. and Hill, J.M.: "Some Theoretical Aspects of Oil Recovery from Fractured Reservoirs," Transactions of Institution of Chemical Engineers (1982) v. 60, 352-358.

27. Killough, J.E. and Kossack, C.A.: "Fifth Comparative Solution Project: Evaluation of Miscible Flood Simulator," Paper SPE 16000 presented at the Ninth SPE Symposium on Reservoir Simulation, San Antonio, TX, February 1-4, 1987.

28. Corbett, K.P.: "Structural Stratigraphy of the Austin Chalk," M.S. Thesis, Texas A&M University, College Station, TX (1982).

29. Poston, S.W.: "Oil Recovery Enhancement from Fractured, Low Permeability Reservoirs," Annual Report, Grant No. DE-FG22-89BC14444, U.S. DOE (Sept. 1990).